



OSMRE National Technology Transfer Team (NTTT), **Applied Science Final Report***
U.S. Department of the Interior, OFFICE OF SURFACE MINING RECLAMATION AND ENFORCEMENT

Spoil Type and Forestry Reclamation Approach Effect on Discharge Water Quality at Reclaimed Surface Mine in West Virginia

OSMRE Cooperative Agreement Number: # S16AC20078
Final Report

Reporting Period (October 1, 2016 – September 30, 2019)

Principal Author(s):

Amir Hass

Jeff Skousen

December 2019

West Virginia State University, Institute, WV 25112

Disclaimer

This report was prepared as an account of work sponsored by an agency of the United States Government. Neither the United States Government nor any agency thereof, nor any of their employees, makes any warranty, express or implied, or assumes any legal liability or responsibility for the accuracy, completeness, or usefulness of any information, apparatus, product, or process disclosed, or represents that its use would not infringe privately owned rights. Reference herein to any specific commercial product, process, or service by trade name, trademark, manufacturer, or otherwise does not necessarily constitute or imply its endorsement, recommendation, or favoring by the United States Government or any agency thereof. The views and opinions of authors expressed herein do not necessarily state or reflect those of the United States Government or any agency thereof.

Abstract

Reclamation of surface mine sites using the Forestry Reclamation Approach (FRA) practices has been shown to improve reforestation success in the Appalachian coalfields. The effect of FRA practices, namely the use of selected sandstone spoils as topsoil substitute material (brown/oxidized vs. gray/reduced sandstone) and placement (loose vs. compacted or deep ripped), on soil water quality were evaluated in a 3-year field study. Experimental plots established in 2005 were instrumented in early 2017 with shallow wells and zero-tension pan lysimeters (at 30 to 80 cm depth) to sample and monitor soil water quality. Water samples were collected weekly after rain events during 2017 - 2019 growing seasons (April to late October) and analyzed for elemental composition; total alkalinity; dissolved organic carbon, and for major ions. Solution pH, temperature, dissolved oxygen, total dissolved solids (TDS), and redox potential were measured *in-situ* in the field before sampling. Results indicated the role of redox-promoted dissolution on soil solution properties and composition. Episodes when TDS exceeded regulatory threshold ($>500 \mu\text{S cm}^{-1}$) were exclusively associated with low redox potential and circumneutral pH. Temporal variations in redox potential govern changes in solution pH, TDS, and overall solution composition. In all, the study emphasized the role of soil biogeochemical processes in governing solution composition (e.g. TDS), and point to the limited capacity of the developing soil to buffer and regulate such processes and outcomes.

Graphical Materials List

Title	Page
Figure 1: Box and Whiskers plot of average solution composition at the different treatment sites during the 3-year project: pH, Eh, Electrical Conductivity (EC), Dissolved Oxygen (DO), and Total Organic Carbon (TOC).	14
Figure 2: Box and Whiskers plot of average solution composition at the different treatment sites during the 3-year project: NH ₄ , NO ₃ , Ca, K, Mg, and Na.	15
Figure 3: Box and Whiskers plot of average solution composition at the different treatment sites during the 3-year project: Fe, Mn, Al, Co, Ni, and Zn.	16
Figure 4: Box and Whiskers plot of average solution composition at the different treatment sites during the 3-year project: P, and S.	17
Figure 5. Temporal changes in Eh, pH, EC, SO ₄ , Alkalinity (and correlation thereof), and in NH ₄ and NO ₃ in Well 1 (Non-compacted Brown site) during the 2017 growing season.	19
Figure 6. Temporal changes in redox potential, pH, and Alkalinity in well 3 (Non-Compacted Brown site), Wells 4 and 5 (Compacted Brown site), and Pan 8 (originally Non-Compacted Gray site) during the 2017 growing season.	20
Figure 7. Temporal changes in Eh, pH, EC, SO ₄ , Alkalinity, Mn, Co, Ni, Zn, and well water level (correlation between pH and Eh for the period between day 253 on; 'E'), in well 6 (compacted Brown site) during 2019 growing season.	23
Figure 8. Correlation between soil solution Eh and total dissolved solids, alkalinity, Mn, and Fe in Brown sites during the 2018 growing season.	24
Figure 9. Relationships between pH and Eh, EC, and Alkalinity during the 2019 (top) and 2018 (bottom) growing.	25
Figure A1: Overall aerial view of the mine site with the locations of non-disturbed, initial site/plots, and the 'new' gray plot.	30
Figure A2: Layout and well locations (yellow pins) at the original brown and gray plots.	31
Figure A3: Layout and well locations at the non-disturbed area.	32
Figure A4: 'New' gray plot with well locations (the red line designates the assigned plot boundary as established by Wilson-Kokes and Skousen, 2014)	33
Figure B1: Acid-ammonium-oxalate (AAO) and Citrate-dithionite (CD) extractable iron in the Brown, Gray and undisturbed / native soil and in gray sandstone quarry rock material (vertical lines are one standard deviation).	36
Figure B2: Acid-ammonium-oxalate (AAO) and Citrate-dithionite (CD) extractable manganese in the Brown, Gray and undisturbed / native soil and in gray sandstone quarry rock material (vertical lines are one standard deviation).	37
Figure B3: Leachate conductivity in the brown (round symbols) or the Gray (triangular symbols) soil during wet/dry cycles column experiment (shaded column represents wet period; vertical lines are one standard deviation).	39
Figure B4: Leachate EC and NH ₄ in the brown (A) or Gray (B) soil during wet/dry cycles column experiment (shaded column represents wet period; vertical lines are one standard deviation; dissected red lines represent 500 or 300 $\mu\text{S cm}^{-1}$).	40

Figure B5: Leachate EC and NO ₃ in the brown (A) or Gray (B) soil during wet/dry cycles column experiment (shaded column represents wet period; vertical lines are one standard deviation; dissected red lines represent 500 or 300 μS cm ⁻¹).	41
Figure B6. Leachate EC and alkalinity in the brown (A) or Gray (B) soil during wet/dry cycles column experiment (shaded column represents wet period; vertical lines are one standard deviation; dissected red lines represent 500 or 300 μS cm ⁻¹).	42

Introduction

Mountaintop removal operations in the central Appalachian region, with an estimated 14.5 million acres being impacted (Pericak et al., 2018), drastically affects the site's and region's ecosystem services (Lindberg et al., 2011; YSEPA, 2011). Given the nature of the operation (i.e. conducted on steep terrain) and the prevailing shallow native soils at these landscapes, regulatory provisions were put in place allowing for the use of topsoil substitutes during reclamation – namely, the use of spent rock material recovered from the stratified geologic formation overlaying the coal seam after blasting and removal during the mining operations. Impediments to reforestation have been poor selection of topsoil substitute material, compaction of that material during placement, and improper choice of vegetation composition. Long-term recovery of ecosystem services to mined sites is dependent on natural vegetation succession and on natural ecosystem restoration processes (Brenner et al., 1984; Burger and Zipper, 2018). The Forestry Reclamation Approach (FRA) was developed in the early 2000's to alleviate those impediments.

The FRA 5-step process provides guidelines to improve reforestation success on reclaimed mine sites in Appalachia (Burger et al., 2005). It aims at developing simple, cost-effective, and easy to implement reclamation practices. The first two FRA steps call for selection of spoil material suitable for hardwood forest establishment and that it be loosely placed to avoid compaction. With loamy textured soils of pH between 5 and 7 and low total dissolved solids identified as the best soil materials for forest growth, it was further recognized that such substitute topsoils can be developed from weathered or unweathered sandstone spoils (especially if mixed with native soils). The use of near-surface, weathered brown sandstone spoils showed over the years to outperform the use of unweathered gray sandstone spoils as topsoil replacement material for reforestation (Emerson et al., 2009; Skousen et al., 2011; Sena et al., 2015; Wilson-Kokes et al., 2013; Sena et al., 2015; Dallaire and Skousen, 2019). In all, FRA practice significantly improves site conditions and plant establishment and growth and as such the practice has been widely adopted by landowners, mine operators, and government agencies (Adams, 2017; Angel et al., 2009).

Inasmuch as the mining activities adversely affect surrounding stream water quality, habitat and biodiversity (Vengosh et al., 2013; Hopkins and Roush, 2013), the effect of FRA practices over the long-term are not well documented. As overburden spoil is placed at the surface as topsoil materials, it is exposed to air and water, promoting further weathering and subsequent release of dissolved solids. The rate and extent of release of dissolved solids from overburden and the specific ions in the percolating waters depend on rock type, particle size distribution, and weathering stage under ambient atmospheric conditions. Recent results from columns and short-term field studies (ca. 2 yr) evaluating the effect of spoil type (e.g. oxidized vs reduced sandstone) on water quality showed that the initial elevated levels of dissolved solids exponentially decreased over time to below the threshold level for stream biota impairment ($500 \mu\text{S cm}^{-1}$), (Agouridis et al., 2012; Orndorff et al., 2015). Furthermore, Evans et al. (2014) predicted that salt concentration in reclaimed areas will decline to natural background levels within 19 years after reclamation. The objective of the study was to determine the effect of FRA practices on soil water quality at a 12-year-old reclaimed mine site.

Executive Summary

Surface mining and poor reclamation practices drastically alter and impair site productivity and ecosystem services, such as clean water. Developing and adopting best reclamation management practices is an essential key for restoration of ecosystem services. Reclamation in the past was often regarded as the least important part of the mining operation and got the least effort of time and money. As such, with more emphasis over the years, reclamation is geared towards active management to achieve short-term regulatory restrictions and bond-release (e.g. percent vegetation cover and erosion control, etc.), while the long-term recovery of the site's ecosystem services relies on natural vegetation succession and on natural ecosystem restoration processes to take place. It is hence of outmost importance to understand how specific reclamation practices and initial sets of conditions affect the long-term development of soil productivity and its capacity to regain, regulate, and sustain ecosystem service processes (e.g. water quality, nutrient cycling, etc.). The Forestry Reclamation Approach (FRA) was established in the early 2000's to develop and promote reforestation reclamation practices. FRA practices were found to significantly improve establishment and growth of forest successional vegetation. While these effects have been extensively studied, the effect of FRA practices on soil biogeochemical processes and on surface and soil water quality are not well documented. The goal of this study was to determine the impact of selected FRA practices on surface and subsoil water quality.

The report summarizes results of a 3-year study of monitoring soil water quality at Forestry Reclamation Approach (FRA) reclaimed sites constructed using different spoil material and compaction relief approaches. The study included Brown (Brwn) and Gray (Gry) Sandstone sites that were compacted or loosely placed during final grading of a reclaimed mine site in southern West Virginia (N38°02'42", W81°30'30"), twelve years prior to instrumenting the sites for this study. Shallow observation wells (1-m deep) were installed in early 2017, and later that year the sites were equipped with additional zero-tension pan lysimeters (at 60 and 30 cm deep). In early 2018, a ripped Gray Sandstone (G-R) site and adjacent undisturbed forest (FS) were instrumented as well. Soil water were monitored and sampled during the 2017 – 2019 growing seasons (early April to mid-November) for composition and solution characterization. This included total alkalinity, ionic composition (Cl, NO₂, NO₃, SO₄, F, Br, PO₄, Li, Ba, K, Mg, Ca, and Na), total and organic carbon, and total elemental analysis (Al, As, Ba, Ca, Cd, Co, Cr, Cu, Fe, K, Mg, Mn, Mo, Na, Ni, P, S, Se, and Zn). Additionally, *in-situ* measurements of pH, TDS, ORP, temperature, and DO were taken at the time of sampling.

The study demonstrated that FRA practice, 12-years after establishment, maintains, on average, suitable soil and surface water quality. On average, total dissolved solids in the different reclaimed sites were below the regulatory threshold of 500, or 300 $\mu\text{S cm}^{-1}$, and decreased in the order: Brwn (282) > Gry (182) \approx FS (211) > Brwn surface runoff water (44 $\mu\text{S cm}^{-1}$). Similarly, the concentration of most of the measured elements, averaged across the 3-year study, were similar to adjacent, non-disturbed forest soil, or comparable to levels in stream waters of non-mined watersheds in the region. Yet, high temporal, in-season, variability was observed for much of the measured parameters; with TDS fluctuating by up to an order of magnitude within a single growing season (from 178 to 1,762 $\mu\text{S cm}^{-1}$). This was especially pronounced in the case of redox-sensitive compounds (e.g. Mn, Fe, NH₄, NO₃). The wide variability and extreme values observed during the study are likely derived from limited ability of the reclaimed soils to properly buffer for moisture (/ gas exchange), pH, and Eh amid temporal changes in environmental / meteorological conditions. Such events and outcomes are discussed in the details of this report. Emphasis is made to highlight

the role of redox-promoted dissolution processes in the monitored systems. This is especially important as much of past attention was directed at acid-promoted dissolution as the dominant process that governed weathering and dissolution processes and solution composition in reclaimed mine sites. With poor separation or inclusion of trace amounts of acid-generating materials (e.g. pyrite minerals) which are ubiquitous to mining operations such emphasis was well deserved. It is likely that better processing of the topsoil substitute spoils, and/or given the stage of soil development (12-15 years after reclamation) led to the current observations and role of redox-promoted dissolution in shaping and controlling solution composition. However, and to the contrary, significant withdrawal of water from the compacted brown site due to unusually dry late summer and fall in 2019 led to sharp decrease in soil pH (from ca. pH 5.8 to 4.3), leading to a rise in TDS and dissolved levels of heavy metals (e.g. Co, Ni, Mn, Zn, etc.). In all, and depending on the prevailing conditions in the soil environment, both acid- and redox-promoted dissolution processes were at play, with limited buffering and regulation by the soil.

The wide and extreme fluctuation in solution properties and composition further pointed to limited soil development processes and to the inability of the developing soil to properly control and regulate biogeochemical processes and outcomes (e.g. TDS levels and composition). We found the brown mine soil to be composed mostly of chemically-weathered materials and for it to be incapable to control and regulate its decomposition. On the other hand, the Gray mine soil was composed mostly of stable non-weathered and poorly-graded blast sandstone rock fragments (pH > 7). This soil seemed to sustain high water infiltration and percolation rates leading to low solution residence time and as such to inhibition of rock weathering, subsequently stalling soil development processes.

Given the composition and use of topsoil substitutes, these limitations and consequences thereof are expected and indeed have manifested themselves in the current study. To mitigate such initial shortfalls, reclamation practices should be aimed at increasing microtopographic heterogeneity. This should include the use of practices such as end-dumping and reduced grading. Such fill placement practices would support the development of microsites of discrete and distinct micro-environments and associated biogeochemical processes (e.g. localities that are very wet, very dry, etc.). Spatial heterogeneity of such microsites would provide for anoxic conditions in depressions and oxic conditions on high points. Such practices would help produce desirable headwater in-stream water quality as the developing soil regains its natural capacity to buffer such conditions and to regulate these processes. Instituting reclamation practices that would help to buffer and regulate such geochemical processes is an important way to improve water quality on surface mines across a variety of weather events.

Experimental

The field study includes plots established in early 2005 on a reclaimed mine site in Kanawha County, about 50 km south of Charleston, WV (38° 5'28" N, 81° 26'37" W). The field study composed of three 2.8-ha plots: one with 1.5 m of weathered brown sandstone, the second had 1.2 m of weathered brown sandstone, and the third had 1.5 m of unweathered gray sandstone. The plots were randomly established on a nearly-level slope adjacent to one another with a 6-m buffer strip between them. After spoil placement, half of each plot was compacted with a D-10 Caterpillar dozer with tracks completely covering the surface, while the other half (non-compacted plot) received only one or two passes with the same dozer (Emerson et al., 2009). The 1.5-m brown and gray sandstone plots were used in this study.

The four plots included in this study composed of Compacted Brown sandstone (BC), Non-compacted brown sandstone (B-NC), Compacted Gray sandstone (GC) and non-compacted gray sandstone (G-NC) plots (See Fig. A1 in Appendix A). The four treatment plots were instrumented each with three shallow observation wells (to a depth of 1.0 m), randomly positioned within each plot, in March 2017. Due to low and infrequent yield of water, mainly in the gray site, a set of zero-tension pan lysimeters were installed at a depth of ca. 60 cm in early June 2017 near the wells of the non-compacted brown and gray sites. Later on during early August 2017 the gray site (both compacted and non-compacted plots) were further instrumented to include pan lysimeters at 30 and 60 cm near each well. As limited and infrequent water yield was still observed at the gray sites, additional gray plot (G-R, see Fig A4 in Appendix A) was instrumented with three clusters of wells and pans in April 2018. At that time, three wells and pans were also installed at a nearby undisturbed forested area to be used as a reference of naturally occurring, non-disturbed forest (see Fig A3 in Appendix A). The soil type at the forest site is a complex of Claymer/Lilly-Dekalb series (loamy, siliceous, semi/active, mesic Typic Hapludults) with a loam/sandy loam A horizon and gradient of increase in active clay content and development of a Bt horizon along the established wells transect. The new Gray plot (ripped area) is located less than half a mile west of the current site and is set within the footprint of the 'GRP' plot set in 2013 by Wilson-Kokes and Skousen (2014). Site preparation at this location was completed in 2005 and the site was ripped in 2011. This addition was made by Wilson-Kokes and Skousen by 2012-2013 due to poor tree survival and growth in the original gray site. Similarly, we decided to monitor this area under the same assumption that it likely better represents the gray sandstone material reclaimed-area. Also, the lower rock and higher fines content (Wilson-Kokes and Skousen, 2014, Table 4 therein) shows a more compatible composition to that of the brown sandstone plot and it is also likely to allow more successful collection of water samples compared to the original gray site. Surface water runoff samples were collected using 500 mL stormwater first-flush Nalgene sampler. Surface runoff samples were collected from the compacted and non-compacted brown plots (See SF-BC, and SF-BNC, respectively in Fig A2 in Appendix A). The stormwater sampling bottles were placed along identified surface runoff/drainage pathway.

The different water sampling devices were visited weekly, annually during the 2017 – 2019 growing seasons (April – Nov). Initially, during March of each year, the wells and pans were cleaned by purging and flushing (the wells were also scrubbed) the devices three times with 0.01M HCl solution. The solutions were pumped back after each purge and the sampling devices were subsequently purged several times with deionized water (DIW) until the backwater reached the original pH of the DIW (ca. 5.6). The cleaning solutions were pumped and collected for further disposal. The storm-water samplers were cleaned and stored in the lab prior to deployment in the

spring. During the sampling season the samplers were replaced each sampling events with cleaned first-flush sampler bottles.

On the weekly sampling during each one of the three the growing season, a multi-parameter multi-probe unite (YSI ‘Pro Plus’, Xylem USA) was first inserted to the well for in-situ measurements of pH, TDS, ORP, temperature, and DO. Solution from the pan sampling devices was pumped by a hand pump to a 500 mL Nalgene bottle prior to YSI measurements in the bottle. Additional water sample was hand pumped from each sampling device and collected into a 500mL Nalgene bottle. The sampled water was pretreated in the field by filtering through 0.45um filter (gridded MCE, MF-Millipore) into 60-mL bottles with minimal headspace for determination of Alkalinity, TOC, and ionic composition. Additional filtered sample was further acidified with concentrated HNO₃ for metal analysis. The samples were placed in iced cooler before being transferred to the lab for analysis. The wells and pans were emptied and capped after each sampling visit.

The collected water samples were brought to WVSVU Soil and Water Laboratory and were analyzed for total alkalinity using Gran-Plot titration assay; ionic composition (Cl, NO₂, NO₃, SO₄, F, Br, PO₄, Li, Ba, K, Mg, Ca, and Na) using ion chromatography (dual Dionex ICS-1100 system); total and organic carbon using TOC Analyzer (OI Analytical, Aurora 1030W); and for total elemental analysis (Al, As, Ba, Ca, Cd, Co, Cr, Cu, Fe, K, Mg, Mn, Mo, Na, Ni, P, S, Se, and Zn) using ICP-OES (Perkin Elmer Optima 8300). Analysis for Alkalinity was done within 24 hours of sampling, ionic and TC analyses were conducted within 24 to 48 hours of sampling, while the acidified sample for ICP analysis was analyzed later on.

In early May of 2018 a weather station was installed at the new gray site (G-R) to monitor meteorological conditions; and in July of that year, 1-m soil moisture access tubes were installed near the wells at the non-disturbed forest, the non-compacted-brown, and the new gray (G-R) sites. A Diviner 2000 soil profile moisture probe (<http://www.sentek.com.au/products/portable.asp>) was used weekly to record soil moisture on a 10-cm interval basis throughout the 1-m soil profile at these locations (the compacted brown site had prevailing excess moisture and access tubes could not be installed).

Results and Discussion

Average soil water composition over the 3-year study are provided in Table 1. Concentration of As, Cd, Cr, Mo, Pb, and Se were below instrument detection limit throughout the 3-year study and are not included in the table (detection limits: As, 0.053; Cd, 0.0034; Cr, 0.0071; Mo, 0.014; Pb 0.042, and Se, 0.075 ppm). Average electrical conductivity (EC), as a measure of the solution total dissolved solids throughout the 3-year study was below the regulatory threshold levels set for decline or chronic aquatic life benchmark values of 500 and 300 $\mu\text{S cm}^{-1}$, respectively (US EPA 2011a, 2011b). Solution EC was significantly higher in the Brown sites than in the Gray ones and decreased in the order (average \pm standard error): Brown sites (282 ± 10) \approx Non-disturbed forest (211 ± 26) $>$ Gray sites (182 ± 15) \gg Surface water ($44.2 \pm 8.9 \mu\text{S cm}^{-1}$; Table 1). Solution pH was significantly lower in the Brown sites (5.96 ± 0.02) compare to the Gray ones (7.20 ± 0.05), which was significantly higher in the Gray than that of the non-disturbed forest (6.85 ± 0.07), while the pH in both the non-disturbed and Gray sites was not significantly different from the pH in the surface runoff water collected in the Brown sites (7.12 ± 0.11).

Overall, average composition of the soil solution in the FRA reclaimed mine sites in this study were similar to that of the non-disturbed forest and to that reported for composition of streams from non-disturbed watersheds in the Appalachian coalfields (US EPA 2011b, Table 2-

4, p.31-34 therein). Yet, the brown sites exhibited significantly lower redox potential and dissolved oxygen content, as well as higher levels of Fe, Mn, Co, and Ni (Table 1), with significant differences in redox potential, Co, EC, and Ni between compacted and non-compacted brown sites (Fig. 1, 3). This suggests that some redox promote dissolution and conditions, occurs in the soil and sustain high levels of redox-sensitive elements in the soil solution (e.g. Fe, Mn), or dissolved products / impurities (Co, Ni) associated with dissolution of such redox-sensitive solid phases/minerals (e.g. free iron/manganese oxides). It is noteworthy that, in comparison to the EPA benchmark for stream water chemistry for streams in non-mined watersheds, both iron and manganese exceeded those levels by several orders of magnitude (compare Table 1 and/or Fig 3 to the Fe and Mn concentration of 0.016 and 0.019 mg L⁻¹, respectively; see Table 4 in US EPA 2011b). However, such elevated levels of redox-sensitive solutes in the soil solution are likely to precipitate out under ambient atmospheric (oxic) conditions once the solution seeps along restrictive subsoil layers out to the surface. Yet, and while atmospheric conditions serve as a barrier for such solutes from penetrating downstream surface waters under the above scenario, further flow thereof down the subsoil and towards replenishment of groundwater can pose problem. Indeed, percolation of soil solution down to groundwater was recently recognized as a major pathway for Mn contamination of groundwater (McMahon et al., 2019). With 300 µg L⁻¹ as a health reference level (US EPA 2003), the average Mn concentration in the brown sites (3.833 mg L⁻¹, Table 1) and/or extreme data point throughout the tested sites, point to potential vulnerability to groundwater.

Furthermore, and as shown in Figures 1 - 4, it is noteworthy that high variability and extreme values in almost all of the measured parameters was observed during the 3-year study, with frequent occurrence of many extreme values, or ‘outliers’ in the Brown sites (outliers – statistically defined as data points that falls beyond 1.5 times the interquartile range [the range where 25 - 75% of the data points falls – the ‘box’ in Figs 1- 4]). Such variability was more pronounced and frequent in the reclaimed sites than in the non-disturbed forest, especially as it relates to components of environmental concern, such as Mn, Fe, Al, Ni, Co (Fig. 3). These extreme values should not be dismissed as outliers, and in fact can be explained in the context of temporal changes in environmental conditions (e.g. soil moisture, temperature, etc.) and in relations to soil biogeochemical processes. As such, these trends and changes reveal important processes associated with the soils ‘parent material’ and pedologic / soil development stage and can help understand and predict solute’s behavior. Such trends and changes are demonstrated below.

Table 1. Site average value of measured parameters across the 3-year study (all treatments per spoil type and all years are pooled together; ‘Surface’ is for surface runoff water collected from the brown sites).

Element / Parameter	Units	Site Type	Avg	SE	Median	Min	Max	Detection Limit
EC	$\mu\text{S cm}^{-1}$	Brown	282 ± 9.90	a [†]	248	18.1	1762	
		Gray	182 ± 14.5	b	127	1.39	683	
		Native	211 ± 25.8	ab	211	31.0	496	
		Surface [‡]	44.2 ± 8.89	c	35.6	9.90	329	
Eh	mV	Brown	288 ± 4.54	b	293	53.8	570	
		Gray	340 ± 5.71	a	338	119	472	
		Native	360 ± 5.71	a	349	309	406	
		Surface	356 ± 7.10	a	352	217	452	
pH		Brown	5.96 ± 0.02	c	5.96	4.26	7.24	
		Gray	7.20 ± 0.05	a	7.22	6.07	8.44	
		Native	6.85 ± 0.07	b	6.94	5.59	7.37	
		Surface	7.12 ± 0.11	ab	7.02	5.95	8.57	
Alkalinity	mg L^{-1} (as CaCO_3)	Brown	68.4 ± 3.86	a	42.7	0.00	691	0.80
		Gray	83.1 ± 7.19	a	60.6	9.62	290	
		Native	97.6 ± 15.3	a	95.2	0.00	280	
		Surface	6.24 ± 0.74	b	5.37	0.69	22.9	
C- TOC	mg L^{-1}	Brown	2.91 ± 0.23	b	0.85	0.00	23.6	0.01
		Gray	3.62 ± 0.46	b	2.07	0.00	29.1	
		Native	6.01 ± 1.36	b	3.38	0.00	15.6	
		Surface	14.0 ± 2.29	a	11.7	3.62	72.8	
DO	mg L^{-1}	Brown	2.07 ± 0.08	c	1.46	0.07	9.08	0.05
		Gray	3.70 ± 0.22	b	3.70	0.56	8.28	
		Native	5.17 ± 0.36	a	5.52	2.06	7.62	
		Surface	3.10 ± 0.38	b	2.69	0.45	11.4	
NH ₄	mg L^{-1}	Brown	0.13 ± 0.04	a	0.00	0.00	6.45	0.10
		Gray	0.00 ± 0.00	a	0.00	0.00	0.00	
		Native	0.00 ± 0.00	a	0.00	0.00	0.00	
		Surface	0.12 ± 0.12	a	0.00	0.00	4.07	
NO ₃	mg L^{-1}	Brown	0.30 ± 0.06	a	0.00	0.00	21.6	0.10
		Gray	0.61 ± 0.10	a	0.31	0.00	5.72	
		Native	0.15 ± 0.04	a	0.11	0.00	1.04	
		Surface	0.50 ± 0.09	a	0.29	0.00	2.68	
Al	mg L^{-1}	Brown	0.128 ± 0.025	a	0.005	0.000	6.323	0.019
		Gray	0.075 ± 0.016	a	0.024	0.000	0.838	
		Native	0.190 ± 0.048	a	0.075	0.000	0.787	
		Surface	0.035 ± 0.005	a	0.031	0.000	0.114	
Ca	mg L^{-1}	Brown	25.9 ± 1.19	b	17.8	0.89	120	0.008
		Gray	16.9 ± 1.28	c	13.1	2.06	47.5	
		Native	43.2 ± 5.89	a	42.0	1.95	124	
		Surface	2.36 ± 0.69	d	1.36	0.40	24.1	
Co	mg L^{-1}	Brown	0.022 ± 0.001	a	0.020	0.000	0.179	0.006
		Gray	0.000 ± 0.000	b	0.000	0.000	0.001	
		Native	0.001 ± 0.000	b	0.000	0.000	0.008	
		Surface	0.000 ± 0.000	b	0.000	0.000	0.000	

Table 1. (Cont.)

Element / Parameter	Units	Site Type	Avg	SE		Median	Min	Max	Detection Limit
Cu	mg L ⁻¹	Brown	0.002	± 0.001	a	0.000	0.000	0.396	0.005
		Gray	0.002	± 0.001	a	0.000	0.000	0.109	
		Native	0.000	± 0.000	a	0.000	0.000	0.000	
		Surface	0.003	± 0.002	a	0.000	0.000	0.056	
Fe	mg L ⁻¹	Brown	5.813	± 0.709	a	0.889	0.000	193.0	0.003
		Gray	0.082	± 0.011	b	0.041	0.000	0.600	
		Native	0.106	± 0.023	ab	0.054	0.004	0.481	
		Surface	0.051	± 0.007	b	0.039	0.006	0.179	
K	mg L ⁻¹	Brown	4.66	± 0.08	a	4.73	1.02	12.5	0.500
		Gray	2.83	± 0.21	b	1.98	0.00	8.98	
		Native	1.64	± 0.26	c	1.10	0.48	6.13	
		Surface	3.08	± 0.41	b	2.35	0.84	12.2	
Mg	mg L ⁻¹	Brown	12.2	± 0.35	a	12.7	0.68	50.9	0.006
		Gray	11.5	± 1.08	a	7.19	1.41	44.2	
		Native	3.89	± 0.44	b	3.48	1.38	10.1	
		Surface	1.89	± 0.55	b	0.95	0.20	19.1	
Mn	mg L ⁻¹	Brown	3.833	± 0.233	a	3.706	0.000	44.87	0.001
		Gray	0.011	± 0.002	b	0.005	0.000	0.153	
		Native	0.041	± 0.009	b	0.027	0.006	0.232	
		Surface	0.056	± 0.014	b	0.025	0.000	0.364	
Na	mg L ⁻¹	Brown	2.45	± 0.19	a	1.07	0.01	26.9	0.026
		Gray	0.60	± 0.06	b	0.40	0.00	4.58	
		Native	1.00	± 0.13	ab	0.87	0.32	3.28	
		Surface	0.26	± 0.03	b	0.23	0.00	0.59	
Ni	mg L ⁻¹	Brown	0.013	± 0.001	a	0.010	0.000	0.152	0.015
		Gray	0.000	± 0.000	b	0.000	0.000	0.005	
		Native	0.000	± 0.000	b	0.000	0.000	0.003	
		Surface	0.001	± 0.000	b	0.000	0.000	0.009	
P	mg L ⁻¹	Brown	0.00	± 0.00	b	0.00	0.00	0.14	0.100
		Gray	0.00	± 0.00	b	0.00	0.00	0.05	
		Native	0.00	± 0.00	b	0.00	0.00	0.00	
		Surface	0.04	± 0.03	a	0.00	0.00	0.44	
S	mg L ⁻¹	Brown	23.5	± 0.72	a	24.1	0.19	95.7	1.000
		Gray	4.10	± 0.47	b	2.58	0.47	19.3	
		Native	4.45	± 0.41	b	4.33	1.78	11.0	
		Surface	1.89	± 0.32	b	1.16	0.25	7.41	
Zn	mg L ⁻¹	Brown	0.030	± 0.008	b	0.012	0.000	2.950	0.001
		Gray	0.006	± 0.001	b	0.003	0.000	0.048	
		Native	0.019	± 0.005	ab	0.012	0.000	0.123	
		Surface	0.102	± 0.021	a	0.037	0.000	0.431	

† Values with the same letter are not significantly different from each other (at p< 0.05)

‡ surface runoff water from Brown sites

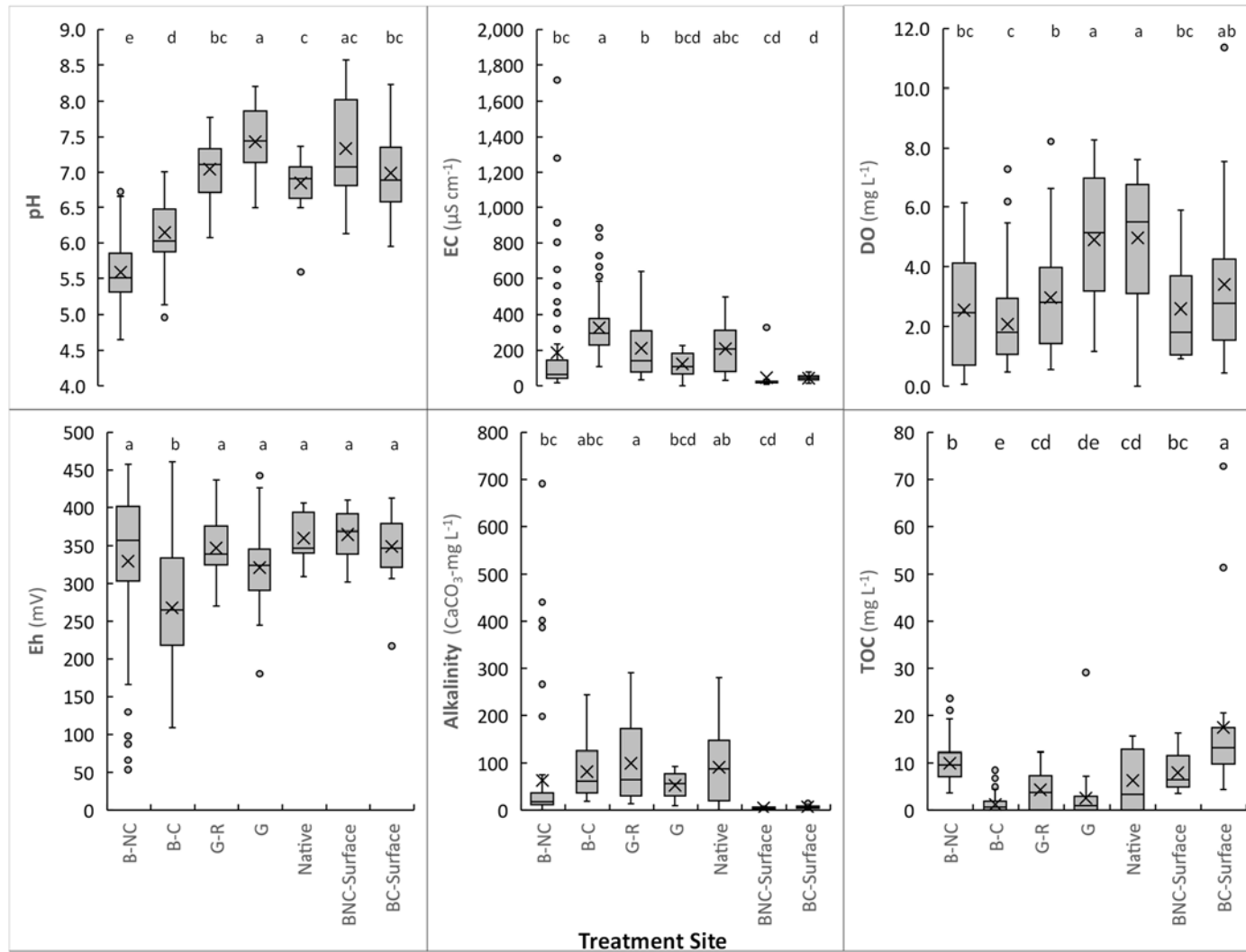


Figure 1: Box and Whiskers plot of average solution composition at the different treatment sites during the 3-year project: pH, Eh, Electrical Conductivity (EC), Dissolved Oxygen (DO), and Total Organic Carbon (TOC). (Brown non compacted, B-NC; Brown compacted, B-C; Ripped Gray site, G-R; original Gray site, G; Non-disturbed forest, Native; Brown non compacted surface runoff, BNC-surface; Brown compacted surface runoff, BC-surface. 'x' symbol – average; Site/treatment followed by the same letter are not significantly different from each other at $p < 0.05$).

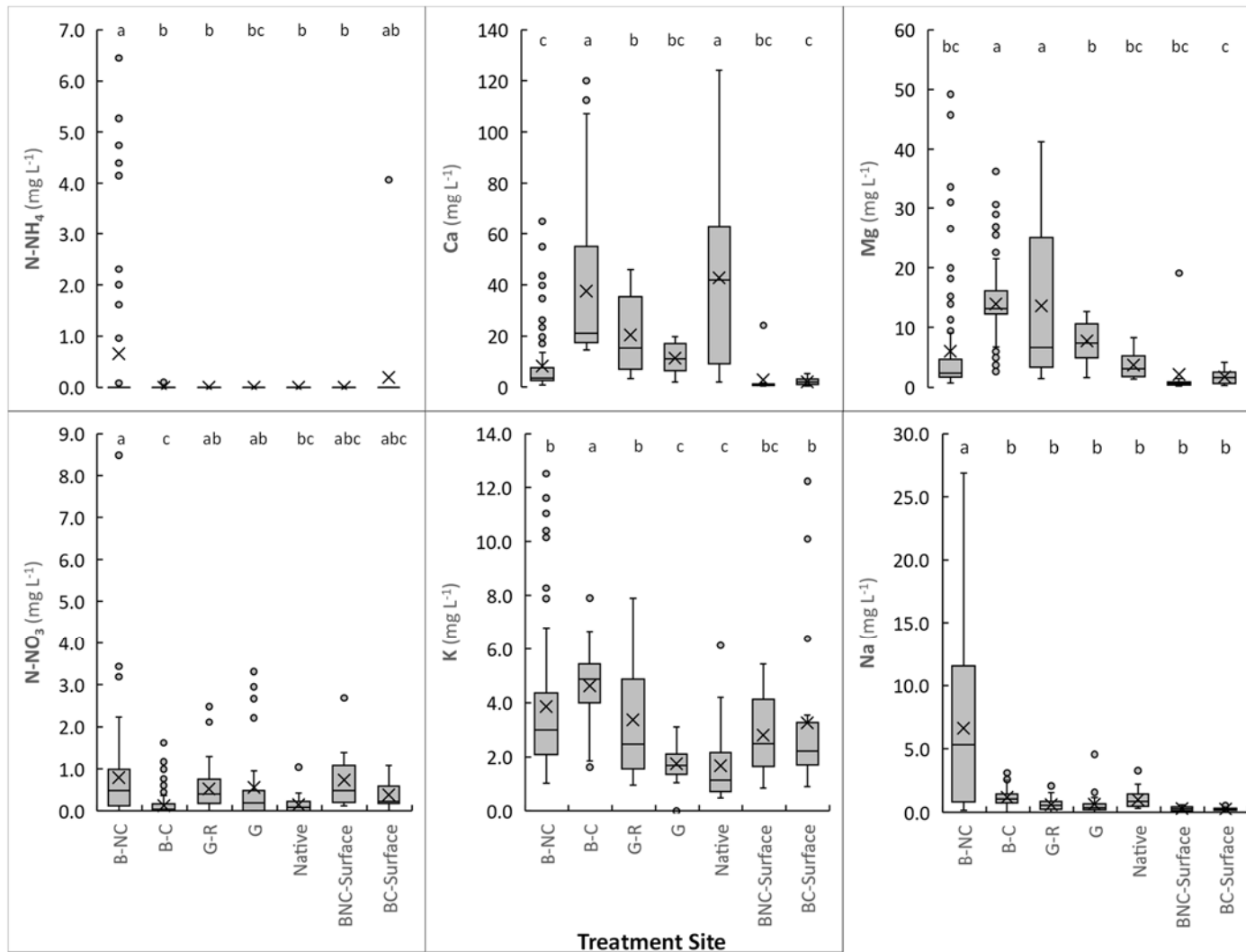


Figure 2: Box and Whiskers plot of average solution composition at the different treatment sites during the 3-year project: NH₄, NO₃, Ca, K, Mg, and Na (Brown non compacted, B-NC; Brown compacted, B-C; Ripped Gray site, G-R; original Gray site, G; Non-disturbed forest, Native; Brown non compacted surface runoff, BNC-surface; Brown compacted surface runoff, BC-surface. 'x' symbol – average; Site/treatment followed by the same letter are not significantly different from each other at p < 0.05).

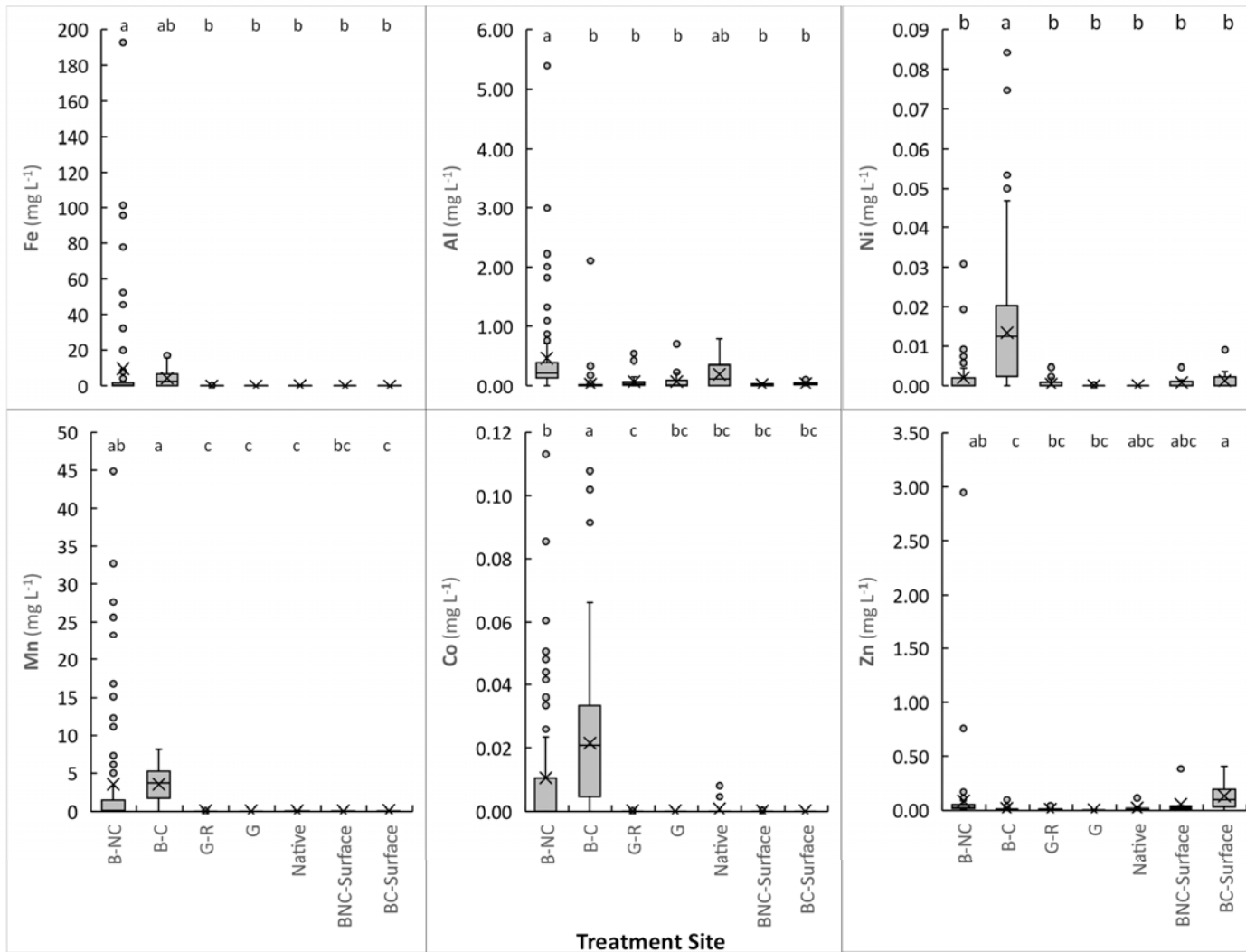


Figure 3: Box and Whiskers plot of average solution composition at the different treatment sites during the 3-year project: Fe, Mn, Al, Co, Ni, and Zn (Brown non compacted, B-NC; Brown compacted, B-C; Ripped Gray site, G-R; original Gray site, G; Non-disturbed forest, Native; Brown non compacted surface runoff, BNC-surface; Brown compacted surface runoff, BC-surface. 'x' symbol – average; Site/treatment followed by the same letter are not significantly different from each other at p < 0.05).

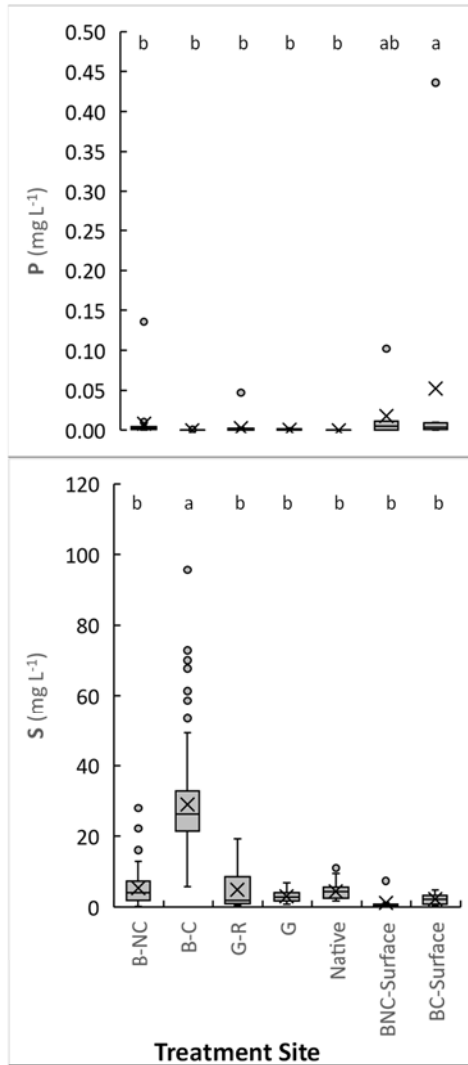


Figure 4: Box and Whiskers plot of average solution composition at the different treatment sites during the 3-year project: P, and S (Brown non compacted, B-NC; Brown compacted, B-C; Ripped Gray site, G-R; original Gray site, G; Non-disturbed forest, Native; Brown non compacted surface runoff, BNC-surface; Brown compacted surface runoff, BC-surface. 'x' symbol – average; Site/treatment followed by the same letter are not significantly different from each other at $p < 0.05$).

Temporal changes in selected solution parameters and dissolved components in Well 1 (Non-Compacted Brown site) during the 2017 growing season is presented in figure 5. Solution pH and Eh varied widely during the growing season (from 6.73 to 5.17, and from 67 to 363 mV, respectively; Fig. 5A) and the two were inversely correlated ($R^2 = 0.92$; Fig. 5E), with the highest Eh values associated with the lowest pH and vice versa (Fig. 5A). While both total dissolved solids (as EC) and alkalinity were also inversely related to Eh, with highest EC and Alkalinity values associated with lowest Eh values (Fig. 5C and 5D), sulfate concentration followed the same trend as Eh, increasing / decreasing with increase / decrease in Eh, respectively (Fig. 5B). These inverse and reciprocal correlation of the two major anions (bi/carbonate [as alkalinity] and sulfate) with solution Eh and EC is presented in Fig. 5F and 5G, respectively. Alkalinity was highly and inversely correlated to redox potential ($R^2 = 0.92$; Fig 5F) and positively correlated with dissolved solids ($R^2 = 0.75$; Fig 5G), while sulfate behaving in an inverse trend with both parameters. These findings point to the fact that episodes of high dissolved solids (EC) were associated with episodes of low redox potential (i.e. low Eh values) and relatively high pH, and that carbonates (as alkalinity) are the dominant anion in the system during those periods (though as being defined by acid titration, any solute that can, during the assay, consume protons is/can be mistakenly accounted for as carbonate). This further suggest that the observed increase in solutes concentration is associated with redox-promote dissolution processes rather than acid-promote dissolution ones dominating the system dissolution processes at that time. Changes in anoxic / oxic redox conditions are also suggested from the behavior of ammonium and nitrate in solution during that time period (Fig 5H). Ammonium concentration increased with decrease in redox potential while nitrate was not detected in solution during that time. Nitrate rather appeared in solution only as redox potential increased later in the season (Fig. 5H), pointing to the different assimilatory/dissimilatory pathways in N cycling and its role as terminal electron acceptor. Similar behavior and trends in pH, alkalinity, and Eh to those observed in Well 1, were also observed in all other treatment / sites during the season and is presented in Figure 6 for additional Non-Compacted Brown (Well 3), Compacted Brown (wells 4 and 5), and for the Non-Compacted Gray site (Pan 8; see also September and December 2017 quarterly reports for additional details and wells).

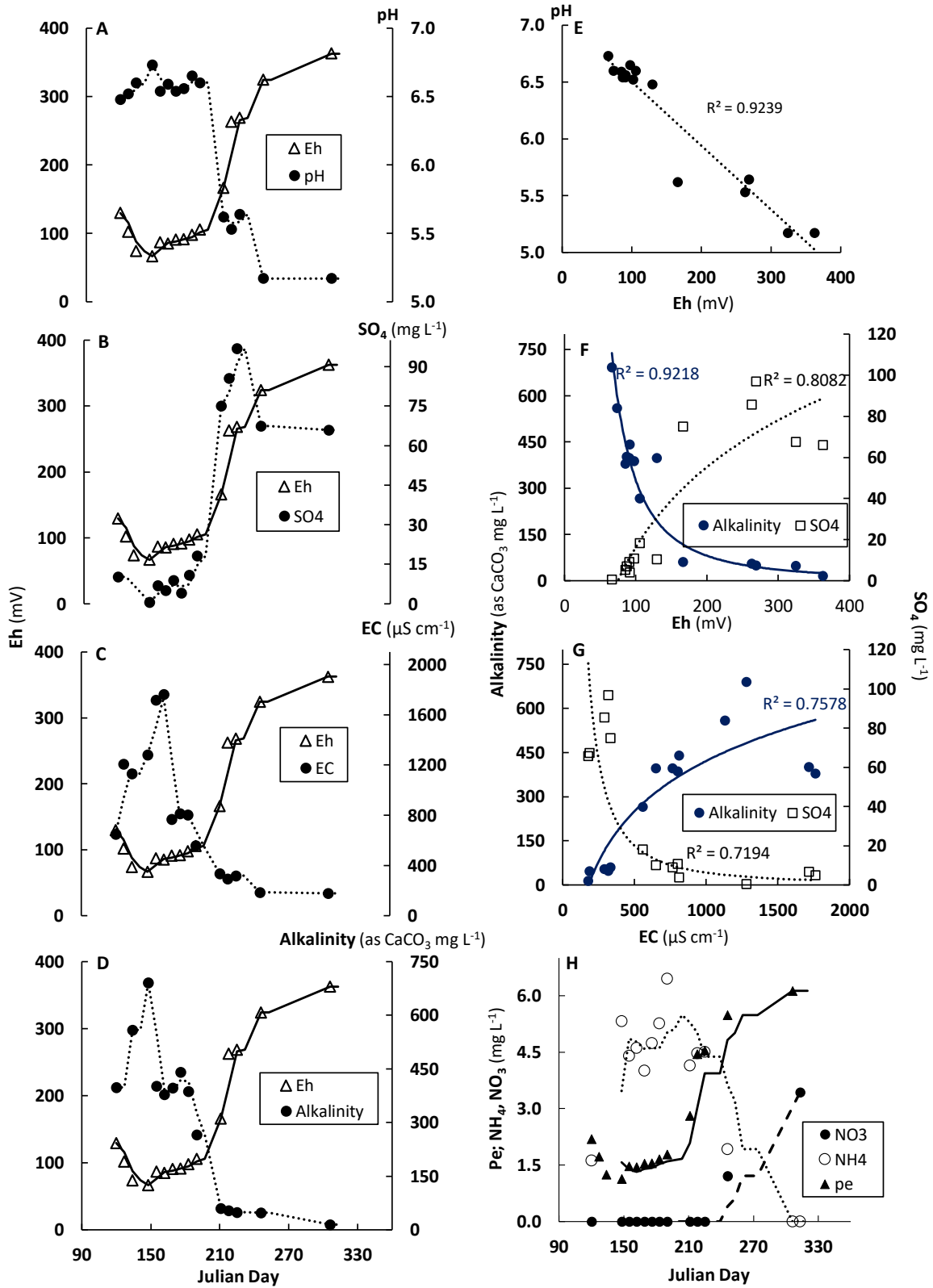


Figure 5. Temporal changes in Eh, pH, EC, SO₄, Alkalinity (and correlation thereof), and in NH₄ and NO₃ in Well 1 (Non-compacted Brown site) during the 2017 growing season.

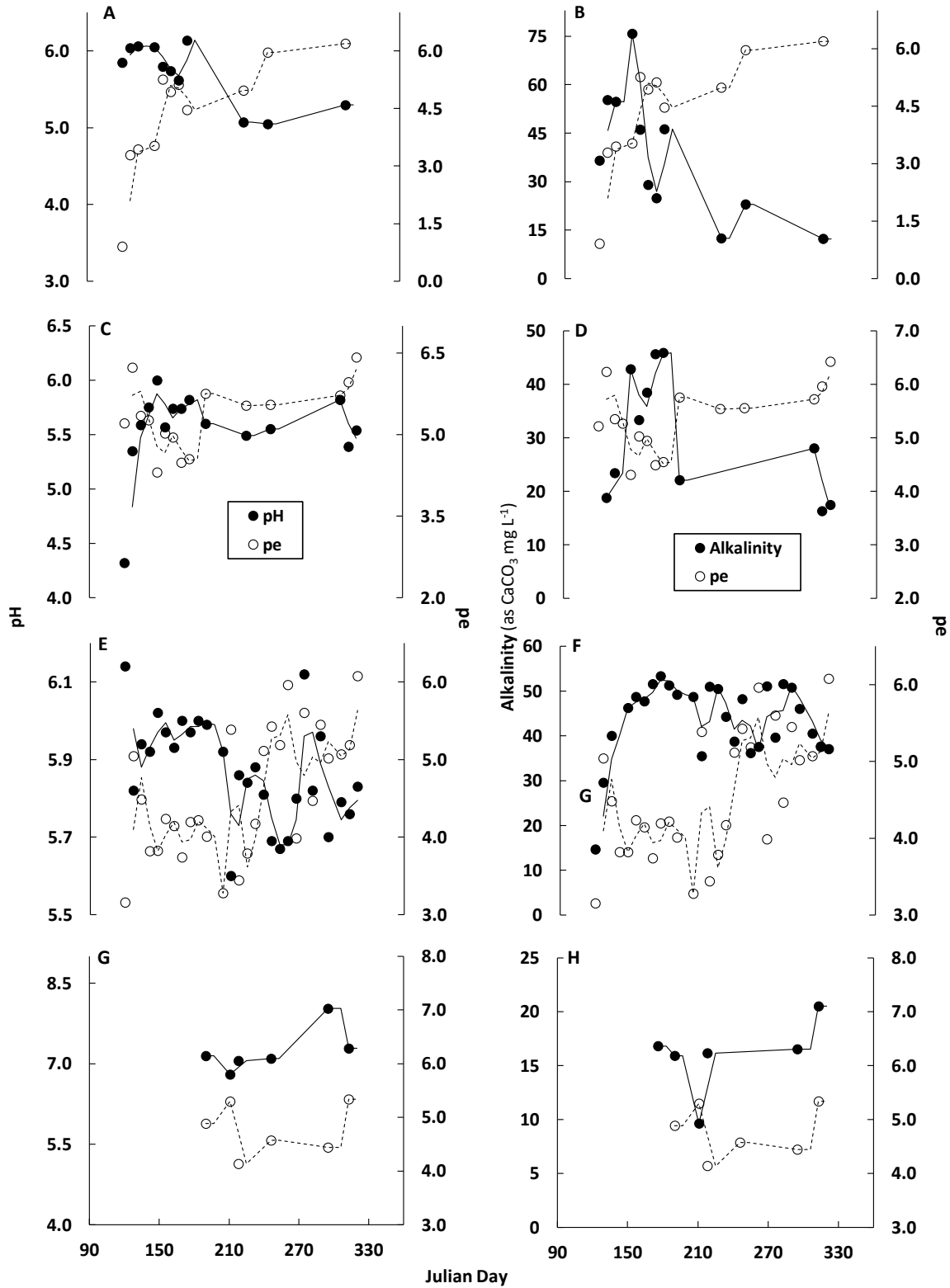


Figure 6. Temporal changes in redox potential, pH, and Alkalinity in well 3 (Non-Compacted Brown site), Wells 4 and 5 (Compacted Brown site), and Pan 8 (originally Non-Compacted Gray site) during the 2017 growing season.

The 2019 growing season, which exhibited hot and dry conditions during the late summer / fall period, provided an additional insight into the chemical behavior of the soil solution in the Compacted Brown site. This was a unique opportunity as this site was consistently and intermittently saturated at the surface throughout the study period, and the dry conditions drove some changes in the site moisture regime/conditions later on in the season. While exhibiting consistent pH and Eh values during mid-season in 2019 (middle range of Fig. 7A), there was a significant decline in pH (from 6.3 to 4.3), and reciprocal increase in Eh (from 237 to 570 mV) from the period between J. Day 253 – 319 (September 10 through November 15; see later part of the 2019 season in Fig. 7A). These changes in pH and Eh were highly and inversely correlated during that time period ($R^2 = 0.88$; Fig. 7E). During that same time EC decrease from a high of $317 \mu\text{S cm}^{-1}$ during mid-season, down to $211 \mu\text{S cm}^{-1}$ by the end of this period (Fig. 7C). Similarly to EC, alkalinity dropped from 70 mg L^{-1} in J. Day 253 down to zero by the end of this period (Fig. 7D). Noteworthy, the behavior of sulfate, alkalinity and total dissolved solids was similar to that observed previously in other wells and periods (i.e. inverse increase in EC and alkalinity with the decrease in Eh [Fig. 7C and FD, respectively], while sulfate increase / decrease with increase / decrease in Eh [Fig &B]).

Solubility of Co, Ni, and Zn which was very low in Well 6 during the 2019 season increased sharply as pH decreased during that late period (Fig. 7F). After an initial decrease, manganese concentration also increased during this time. This may reflect some dynamic (dis)equilibrium and reaction kinetics as the rise in Eh may resulted in oxidation of reduced soluble Mn and precipitation thereof (can account for the observed initial sharp decline in Mn – Fig7F), following by acid dissolution of Mn-associated/bearing minerals with the subsequent/ in-tandem decrease in pH (accounting for the subsequent increase in Mn; Fig. 7F). These sudden changes in solution chemistry occurred as water level in the well drops from an average of 26 cm below the surface during the period preceding September 10, down to the point where no free water were detected in the 100 cm deep well (October 1st through October 9th, 2019; rainfall replenished soil water levels later on – see Fig. 7G). It is likely that such sharp changes in environmental conditions, from a consistent saturated pore space state to a rather sharp withdrawal and reduction in gravitational water content that led to increase in soil pore aeration and subsequent change in redox potential, etc. Noteworthy, daytime temperature during this period were uncharacteristically high (in the mid 30's °C), reaching at times 39 and 40 °C, allowing intensive microbial activity response to the marked decline in water level and changes in oxic/anoxic conditions. Given the increase in intensity and uncertainty associated with climatic and temporal weather/meteorological conditions, it is highly important to fully understand the impact of management practices on the ability of the system to response, buffer, and mitigate such induced changes on the soil environment. As the gray sites are constructed from rock formations that were originally buried deeper in the vertical rock layer stratification were less exposed to the ambient atmospheric conditions, and as such would expected to be less stable (and more weatherable). This was not the case and the gray sites seemed to be stable and less susceptible to increase in dissolved solids. Although not explored in this study, it is likely that settled differences (to routine physical soil analyses) in texture, structure, rock size and specific surface area, as well as other physical and hydrological conditions led to rapid dissipation of water in the gray sites leading to low residence time of the solution in the 'soil' media. This in turn can lead to kinetic inhibition of weathering process and progress which is dependent and associated with the solubility and rate of dissolution of the mineralogical makeup

of the media. Composed of rather stable mineralogy, residence time is known to markedly affect the dissolution of rock formations, such as sandstone (Walling 1980; Appelo and Postma, 2005).

Similar behavior between the measured components and Eh that was found in the 2017 and 2019 growing season occurred also during the 2018 one as shown for the brown sites in Figure 8. Both pH, Fe, Mn, Alkalinity and total dissolved solids were negatively associated with Eh, increasing with the decreasing in soil solution redox potential. Contrary to this trend, Al concentration was positively associated with Eh, increasing with increase in Eh (Fig. 8B). This is likely due to decrease in pH, which was shown to be associated with the increase in Eh (Fig. 8F), and is known to affect Al solubility (i.e. increase in solubility with decrease in pH; Lindsay and Walthall, 1996). Unlike in Well 1 in 2017 (Fig. 5G), results from 2018 suggests similar trend and contribution of sulfate and alkalinity to total dissolved solids (Fig. 8D, and 8H). Given the much lower prevailing Eh in Well 1 during 2017 (and much higher EC), these differences likely associated with reaching (or not) of equilibrium threshold associated with the competing processes (noteworthy, there was no apparent differences between S and SO₄, both of which were simultaneously determined on these samples).

As was shown and discussed above, solution pH shifted towards higher values and circumneutral pH with decrease in Eh. As more pronounced the changes in the Brown treatment sites were, so were the inverse trends between Eh and pH (see Fig 5A for Well 1, Fig 6A for Well 3[also non-compacted brown], and Fig. 7A for Well 6). Yet, and to a lesser extent, such relationships were noted also for the Gray site (Fig 6G). This trend of shifting in pH towards circumneutral values with increasing anoxic conditions and equilibrium thereof, is a well-known phenomenon, documented mostly in wetland environments (see Reddy and DeLauna 2008, and references therein).

Pooling the 2018 and 2019 seasonal datasets (Fig. 9), the convergence and decrease of the spread in the Eh, EC and alkalinity datasets as that of pH converges towards circumneutral values is very noticeable. The increase in total dissolved solids towards values exceeding the 500 and 300 $\mu\text{S cm}^{-1}$ threshold levels were associated with a reciprocal trend of decreasing Eh values, as solution pH neared circumneutral values (i.e. notice the upward / downward cone-shape of the EC / Eh data clouds, respectively, in Fig. 9).

The inverse relationships of nitrate (as indicator proxy for redox potential) and/or inundation periods with high total dissolved solids were also demonstrated in a column experiment conducted under induced wet/drying conditions of gray and brown topsoils collected from the study sites (See June 2019 quarter report in Appendix B). Chemical analysis of the soils further showed very low levels of free iron oxides (determined by Citrate-Dithionite-extraction; Loeppert and Inskeep, 1996; Appendix B). This limited pool of redox-sensitive minerals suggests limited soil poisoning / buffering capacity towards redox potential under development of anoxic conditions.

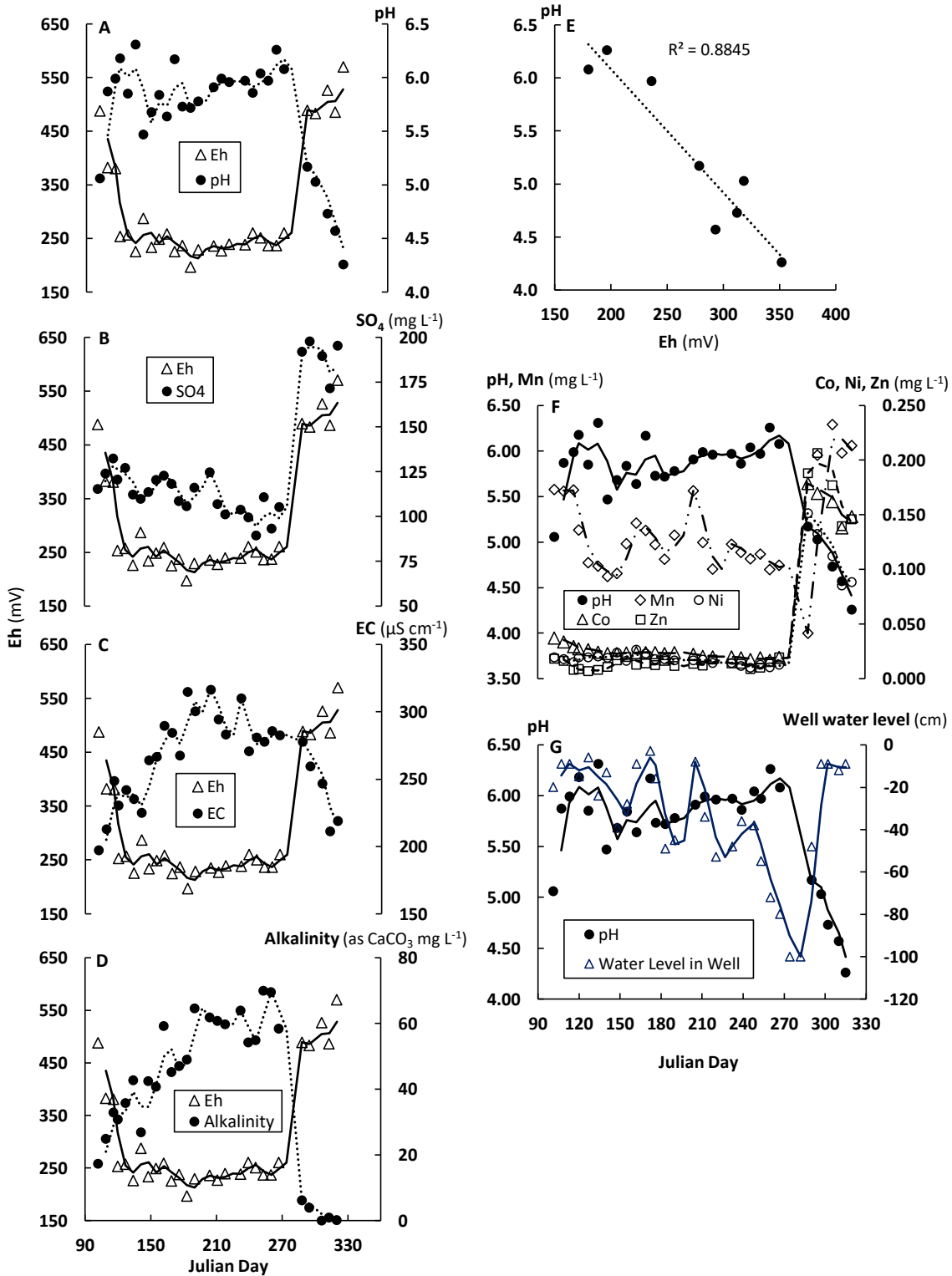


Figure 7. Temporal changes in Eh, pH, EC, SO_4 , Alkalinity, Mn, Co, Ni, Zn, and well water level (correlation between pH and Eh for the period between day 253 on; 'E'), in well 6 (compacted Brown site) during 2019 growing season.

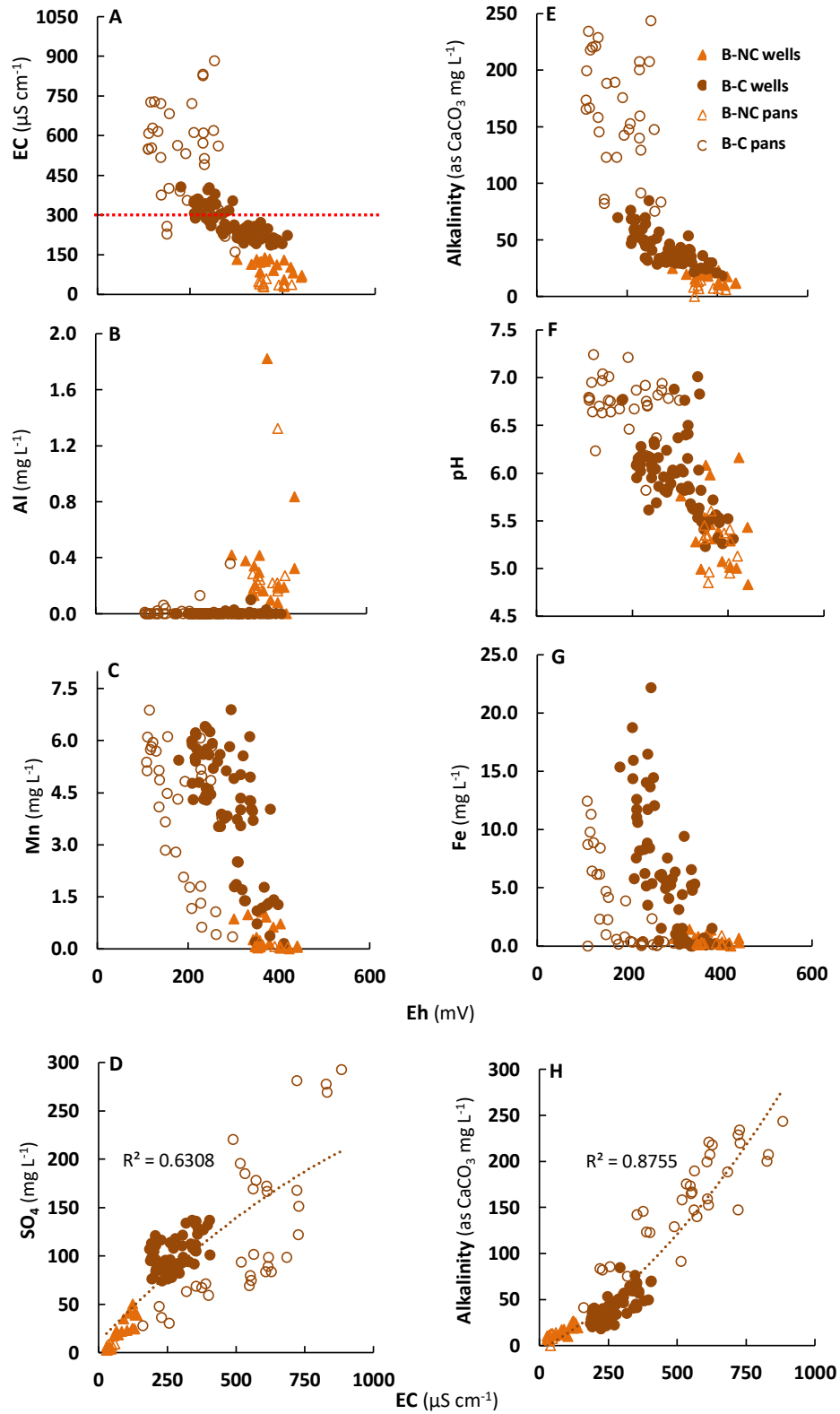


Figure 8. Correlation between soil solution Eh and total dissolved solids, alkalinity, Mn, and Fe in Brown sites during the 2018 growing season (the dashed horizontal red line represent the 300 $\mu\text{S cm}^{-1}$ chronic aquatic life threshold benchmark value).

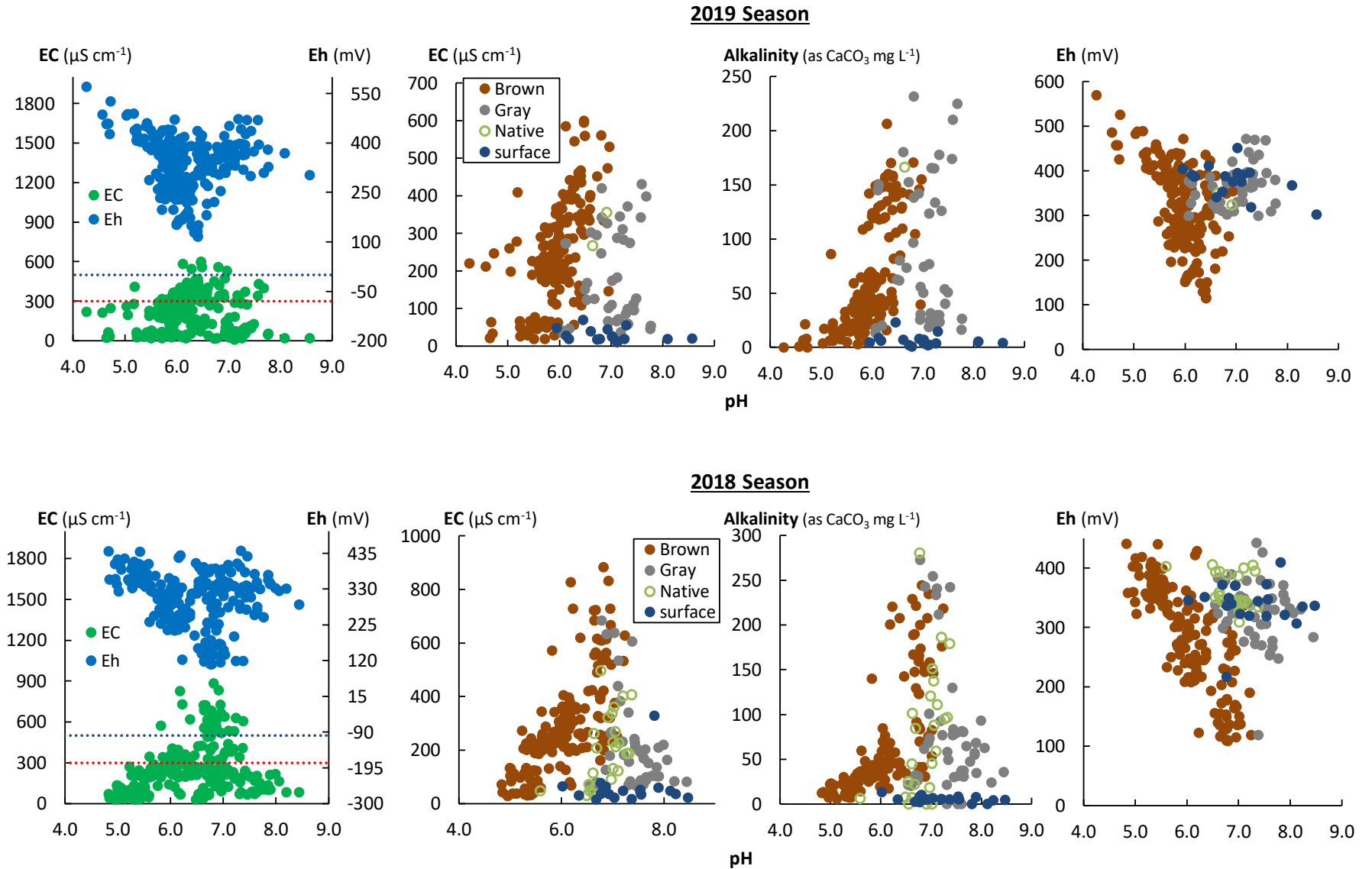


Figure 9. Relationships between pH and Eh, EC, and Alkalinity during the 2019 (top) and 2018 (bottom) growing season ('surface' is surface runoff water, dissected blue and red lines represent 500, and 300 $\mu\text{S cm}^{-1}$ threshold values for decline or chronic aquatic life benchmark, all respectively).

Conclusion

The 3-year study demonstrated that FRA practice, 12-years after establishment, maintains, on average, suitable soil and surface water quality. Yet, high variability and extreme values (mainly of redox-sensitive elements, such as Fe and Mn) was observed during the growing season of all three years. Very early stages of soil development are a prevalent condition expected from such reclaimed mine sites, especially if/when constructed using high proportion of topsoil-substitute, namely crushed rocks recovered from blasting of near-surface rock formations during the mining operations. While ‘historic’ practices, where acid forming materials were ubiquitous to the reclaimed surface fill material, rightfully directed much deserved attention to acid-promote dissolution processes, this study point the attention to redox-promote dissolution as equally deserved phenomenon to be considered in construction and management of such sites and soils.

The study points to vulnerabilities associated with poorly buffered biogeochemical processes, in promoting both acid, and redox promote dissolution. Most of the events were dissolved solids exceeded regulatory thresholds were associated with low redox potential. Subsequent soil analysis and incubation studies pointed to the material limited pools of redox-sensitive minerals (i.e free oxides of Fe and Mn), and demonstrated the important thereof (and that of other terminal electron acceptors along the redox ladder) in affecting and poisoning soil redox potential, especially in the presence of high sulfate levels which are ubiquitous to reclaimed mine sites/soils.

The gray and brown topsoil substitute materials in this study could be seen as the end-members along the continuum of regolith to saprolite rock material (loosely defined here as physically, and chemically weathered rocks, respectively). It is important to balance the mixing of the two, along with that of the remnants of the native soil, and to follow the loosely placement practices of FRA in order to give a good starting point for the developing soil to establish and develop texture structure and mineral and organic pools to further develop and buffer soil moisture nutrient and energy cycles. This is especially important amid increase in frequency and intensity of extreme weather events. The interlocking staggered loosely dumped spoil placement practice of FRA (i.e. end-dumping, or reduce grading) seemed to create heterogeneous micro-topography. This is likely to further diversification and heterogeneity of microsites environmental conditions, promoting biogeochemical processes that in turn may subsequently cancel each other, resulting in (pseudo) buffering of the system on the site scale basis, and likely to favorably affect in-stream water quality. This is likely to buy time for regulating and sustaining water quality and other ecosystem services as pedogenic processes progresses and sustainable soil buffering capacities (for moisture, pH, Eh, etc.) ensue.

References

- Adams M.B. (ed). 2017. The Forestry Reclamation Approach: Guide to Successful Reforestation of Mined Lands. USDA Forest Service, Northern Research Station. General Technical Report NRS-169 DOI: <https://doi.org/10.2737/NRS-GTR-169>
- Agouridis, C.T., P.N. Angel, T.J. Taylor, C.D. Barton, R.C. Warner, X. Yu, and C. Wood. 2012. Water quality characteristics of discharge from reforested loose-dumped mine spoil in Eastern Kentucky. *J. Environ. Qual.* 41:454–468.
-

- Angel P.N., J.A. Burger, V.M. Davis, C.D. Barton, M. Bower, S.D. Eggerud, and P. Rothman. 2009. The forestry reclamation approach and the measure of its success in Appalachia. *Proceedings American Society of Mining and Reclamation*, 2009 p 18-36 DOI: <http://10.21000/JASMR09010018>.
- Appelo C.A.J., and D. Postma. 2005. *Geochemistry, groundwater and pollution*. 2nd edition. CRC Press.
- Brenner F.J., M. Werner and J. Pike. 1984. Ecosystem development and natural succession in surface coal mine reclamation. *Minerals and the Environment*. 6(1):10-22.
- Burger J.A., and C.E. Zipper. 2018. *How to restore forests on surface-mine land*. Virginia Cooperative Extension Pub. 460-123, Virginia Tech.
- Burger, J., D. Graves, P. Angel, V. Davis, and C. Zipper. 2005. The forestry reclamation approach. *Appalachian Regional Reforestation Initiative. Forest Reclamation Advisory No. 2*, December 2005.
- Dallaire K., and J. Skousen. 2019. Early Tree Growth in Reclaimed Mine Soils in Appalachia USA. *Forests* 10, 549; <http://doi:10.3390/f10070549>
- Emerson P., J. Skousen, and P. Ziemkiewicz. 2009. Survival and Growth of Hardwoods in Brown versus Gray Sandstone on a Surface Mine in West Virginia. *J. Environ. Qual.* 38:1821–1829.
- Hopkins, R.L., and J.C. Roush. 2013. Effects of mountaintop mining on fish distributions in central Appalachia. *Ecol. Freshwater Fish.* 22(4): 578–586.
- Lindsay W.L., and P.M. Walthall. 1996. The solubility of aluminum in soils. p.333-362, In: G. Sposito (ed.) *The environmental chemistry of aluminum*. 2nd ed. Lewis Publishers, Boca Raton, FL.
- Loeppert R.H., and W.P. Inskeep. 1996. Iron. p. 639-664 In: D.L. Sparks et al., (Eds) *Methods of soil analysis, Part 3 chemical methods*. SSSA, ASA, Madison WI
- McMahon, P.B., K. Belitz, J.E. Reddy, and T.D. Johnson. 2019. Elevated Manganese Concentrations in United States Groundwater, Role of Land Surface–Soil–Aquifer Connections. *Environ. Sci. Technol.* 53:29–38.
- Orndorff, Z.W., W.L. Daniels, C.E. Zipper, M. Eick, and M. Beck. 2015. A column evaluation of Appalachian coal mine spoils' temporal leaching behavior. *Environmental Pollution* 204: 39-47.
- Reddy K.R., and R.D. DeLaune. 2008. *Biogeochemistry of wetlands, science and applications*. CRC Press.
- Sena, K., C. Barton, S. Hall, P. Angel, C. Agouridis, and R. Warner. 2015. Influence of spoil type on afforestation success and natural vegetative recolonization on a surface coal mine in Appalachia, United States. *Restoration Ecology*, 23(2): 131–138.
- Skousen, J., C. Zipper, J. Burger, C. Barton, and P. Angel. 2011. Selecting materials for mine soil construction when establishing forests on Appalachian mine sites. *Forest Reclamation Advisory No. 8*, July 2011.
- Tabari H., M.E. Grismer, and S. Trajkovic. 2013. Comparative analysis of 31 reference evapotranspiration methods under humid conditions. *Irrig. Sci.* 31(2):107–117.
- U.S. EPA. 2003. Health effects support document for manganese. EPA 822-R-03-003.
- U.S. EPA. 2011a. *A Field-Based Aquatic Life Benchmark for Conductivity in Central Appalachian Streams*. Office of Research and Development, National Center for Environmental Assessment, Washington, DC. EPA/600/R-10/023F.
-

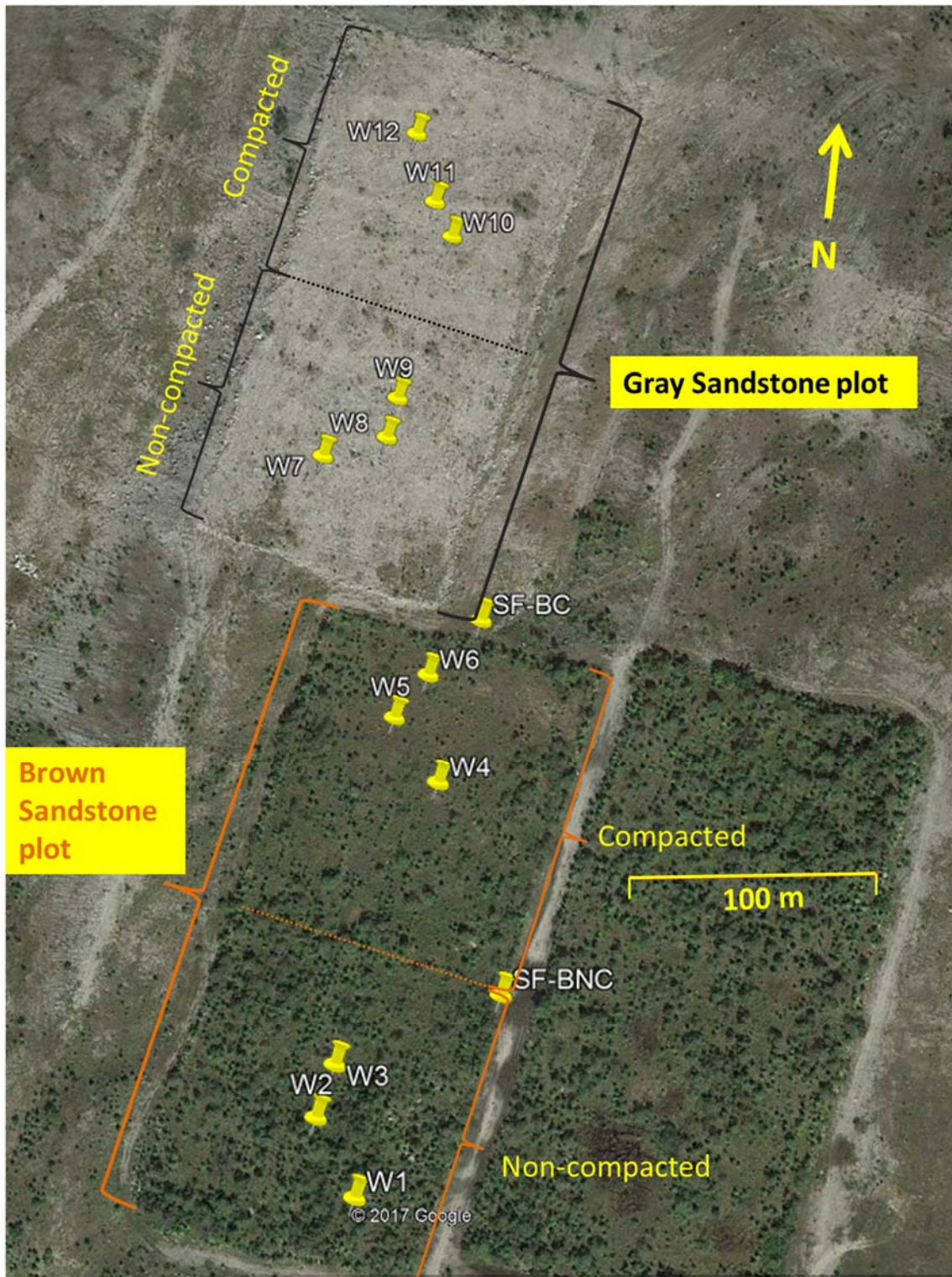
- U.S. EPA 2011b. The Effects of Mountaintop Mines and Valley Fills on Aquatic Ecosystems of the Central Appalachian Coalfields. Office of Research and Development, National Center for Environmental Assessment, Washington, DC. EPA/600/R-09/138F.
- Vengosh, A., T.T. Lindberg, B.R. Merola, L. Ruhl, N.R. Warner, A. White, G.S. Dwyer, and R.T. Di Giulio. 2013. Isotopic Imprints of Mountaintop Mining Contaminants. *Environ. Sci. Technol.* 47 (17): 10041–10048.
- Walling D.E., 1980. Water in the catchment ecosystem. p. 1-48, *In* A.M. Gower (ed.), *Water quality in catchment ecosystems*. Wiley and Sons, New York.
- Wilson-Kokes, L., P. Emerson, C. DeLong, C. Thomas, and J. Skousen. 2013. Hardwood tree growth after eight years on brown and gray mine soils in West Virginia. *J. Env. Qual.* 42: 1353-1362. <https://DOI10.2134/jeq2013.04.0113>.
- Wilson-Kokes, L., and J. Skousen. 2014. Tree growth on ripped, compacted, and slightly compacted gray sandstone topsoil substitute on a surface coal mine in West Virginia. *JASMR*, 3(1): 117-136.
-

Appendix A

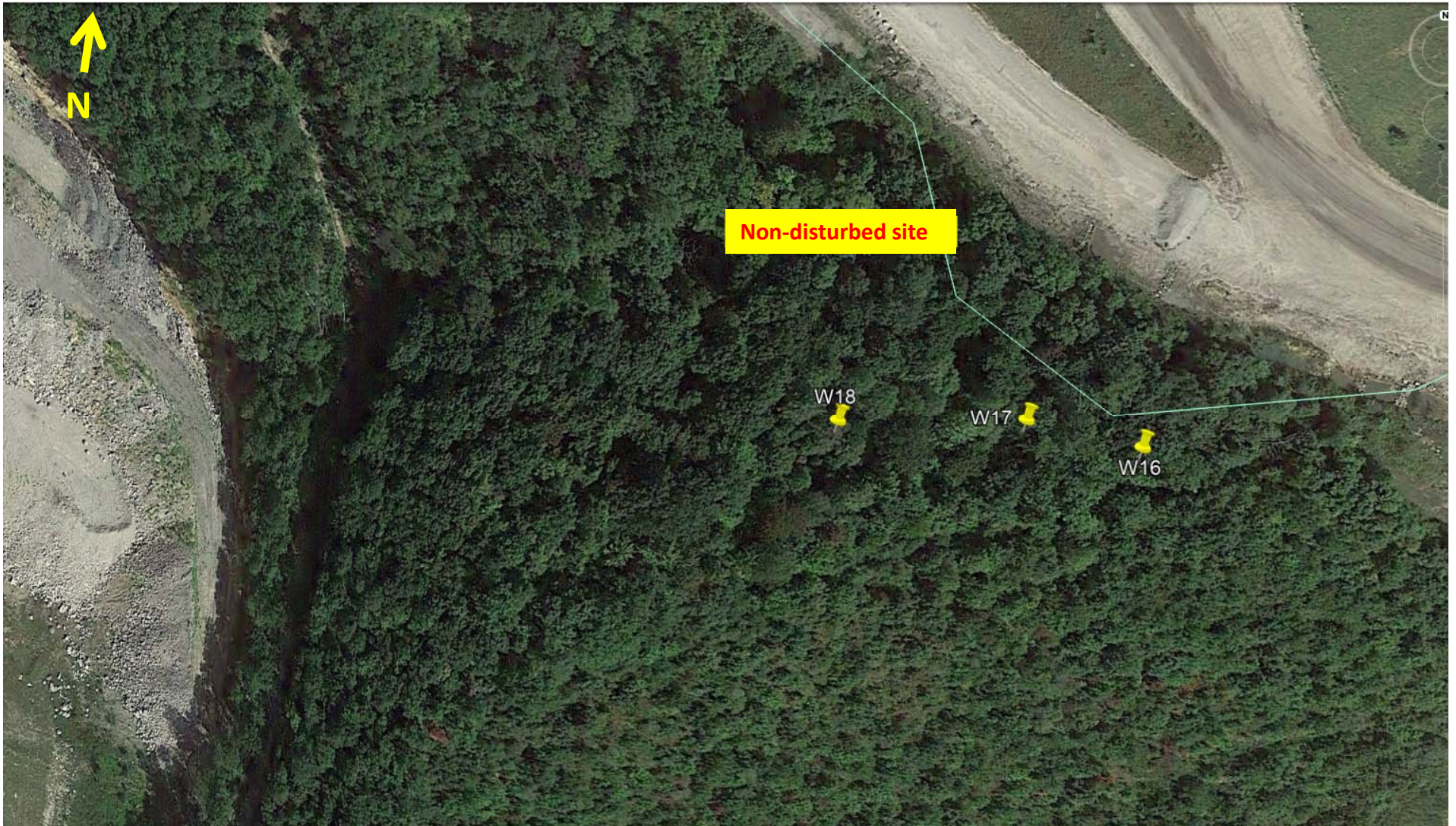
Experimental Site Layout



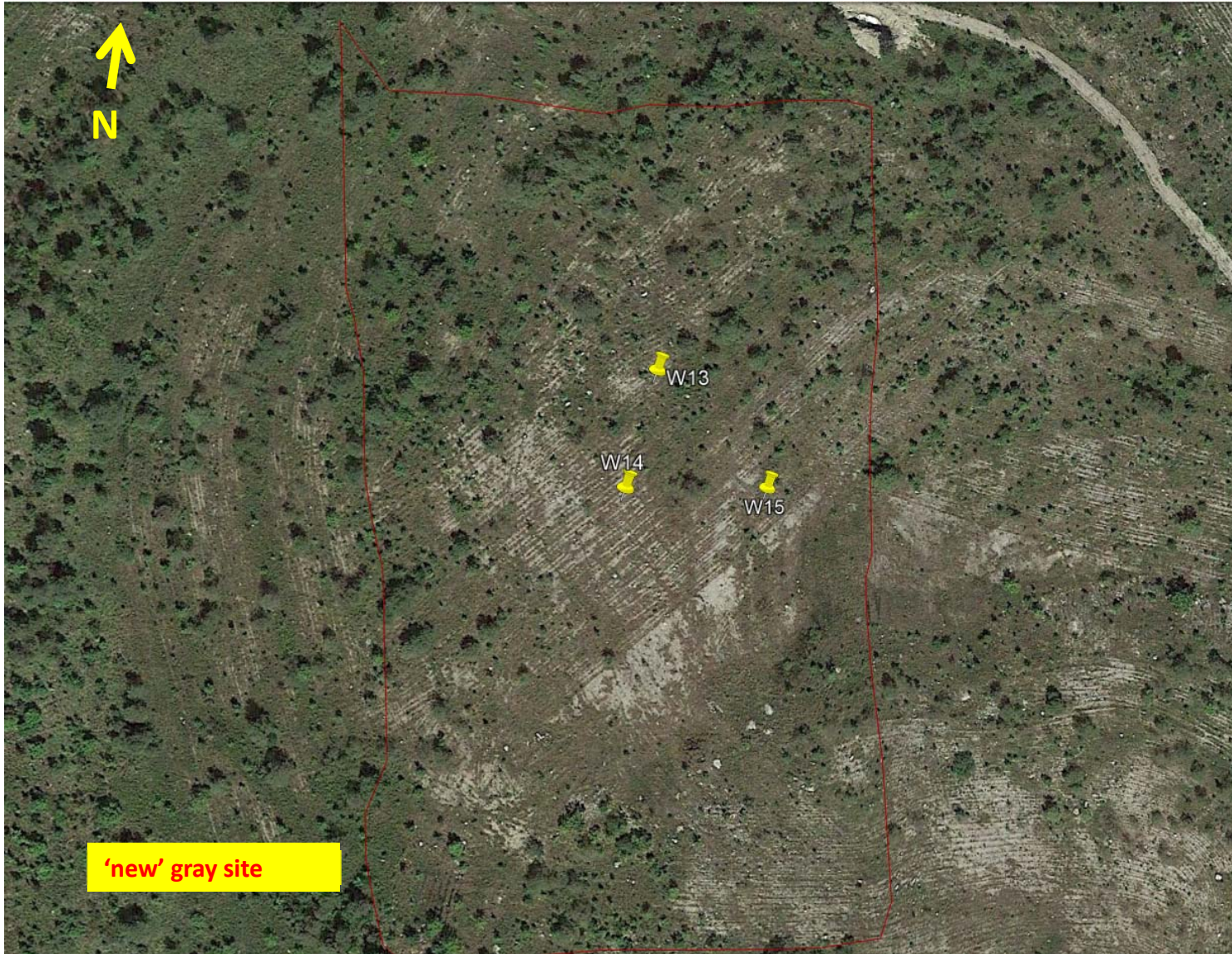
A1: Overall aerial view of the mine site with the locations of non-disturbed, initial site/plots, and the ‘new’ gray plot (GR; yellow pins represent individual well location; red line represent 100 m scale; red lineout at the ‘new’ gray represents the plot boundaries).



A2: Layout and well locations (yellow pins) at the original brown and gray plots.



A3: Layout and well locations at the non-disturbed area.



A4: 'New' gray plot with well locations (the red line designates the assigned plot boundary as established by Wilson-Kokes and Skousen, 2014).

Appendix B

June 2019 Quarter Report

June 2019

Summary of this Quarter's Activities

Water sampling and monitoring resumed on April 8 and continued on a weekly basis thereafter. Mine soils were analyzed for total free oxide minerals of iron and manganese and these pools, especially the well-crystalized ones seemed to be very low, though as expected for such young “soils”. Results of a 53-week long soil column experiment are reported and finding are in accord with field findings where high EC in soil leachate is associated with saturated / anoxic conditions. Appendix A includes the experimental sites layout; Appendix B includes an inventory of all water sampling devices and soil profile moisture access tubes prepared and used in the 2019 sampling season.

Technical Progress

Site activities and water monitoring and sampling

Water sampling and soil moisture monitoring resumed on the week of April 8 and is continued on a weekly basis since, using YSI multi probe for in-situ monitoring of soil water EC, DO, ORP, Temp. and pH. Collected samples analyzed for major ion and total metal composition (using ion chromatography and ICP-OES, respectively) as well as for alkalinity, and total, inorganic, and organic carbon. Samples and data are at various on-going stages of processing and analysis.

Free iron and manganese oxides in the Brown, Gray and native soils

Single selective extraction of acid ammonium oxalate [AAO], and Citrate-dithionite [CD] are soil extractions used in the determination soil iron poorly crystalized (e.g. Ferrihydrite, etc.), and total / well crystalized free iron oxides (e.g. hematite, goethite), respectively (Loeppert and Inskeep, 1996). These assays are commonly used for soil characterization and classification as these pools size and vertical distribution within the soil profile are indicative of soil formation and development stage, as well as for soil horizon determination stratification and classification (e.g. B_t horizon). We used these assays here to quantify the pools of the soils major free oxides that are redox sensitive (i.e. iron and manganese oxides; which, unlike aluminum oxides are subject and sensitive to redox dissolution processes). Surface soil samples from all three soil types (undisturbed, Gray and Brown sandstone), as well as a sample from a crushed gray sandstone rock formation from a local quarry were finely ground and pass through 2mm sieve prior to analysis. AAO extraction is based on acid and ligand-promote dissolution and is conducted in acidic medium environment (pH 3.15), while CD rely mainly on redox-promoted / reductive dissolution (dithionite) of free ferric oxides and is conducted at pH of 6.5. The latter also include ligand (citrate) that contribute to dissolution via ligand-promote dissolution but is mainly act as a sink for the released iron to reduce its activity and keep the dissolved iron in solution.

AAO and CD-extractable iron and manganese are presented in figures B1 and B2, respectively. CD extractable iron was higher than that of AAO in both the brown and native soil. This trend (i.e.: $Fe_{CD} > Fe_{AAO}$) is consistent with observations in natural soil systems where quasi steady-state prevails, leading to the formation and high proportion of stable well-crystalized iron oxides minerals (e.g. hematite, goethite) over poorly crystalized unstable ones (e.g. ferrihydrite).

However, overall levels of CD and AAO-extractable iron were on the low end of what is commonly found in upland soils (usually > 0.2%, or >2,000 mg kg⁻¹). This suggests that both the brown and the native soil are of low levels of free iron oxides which is expected in sandy and/or newly developed soil systems. Surprisingly, AAO extractable iron was higher than CD extractable iron in the Gray soil.

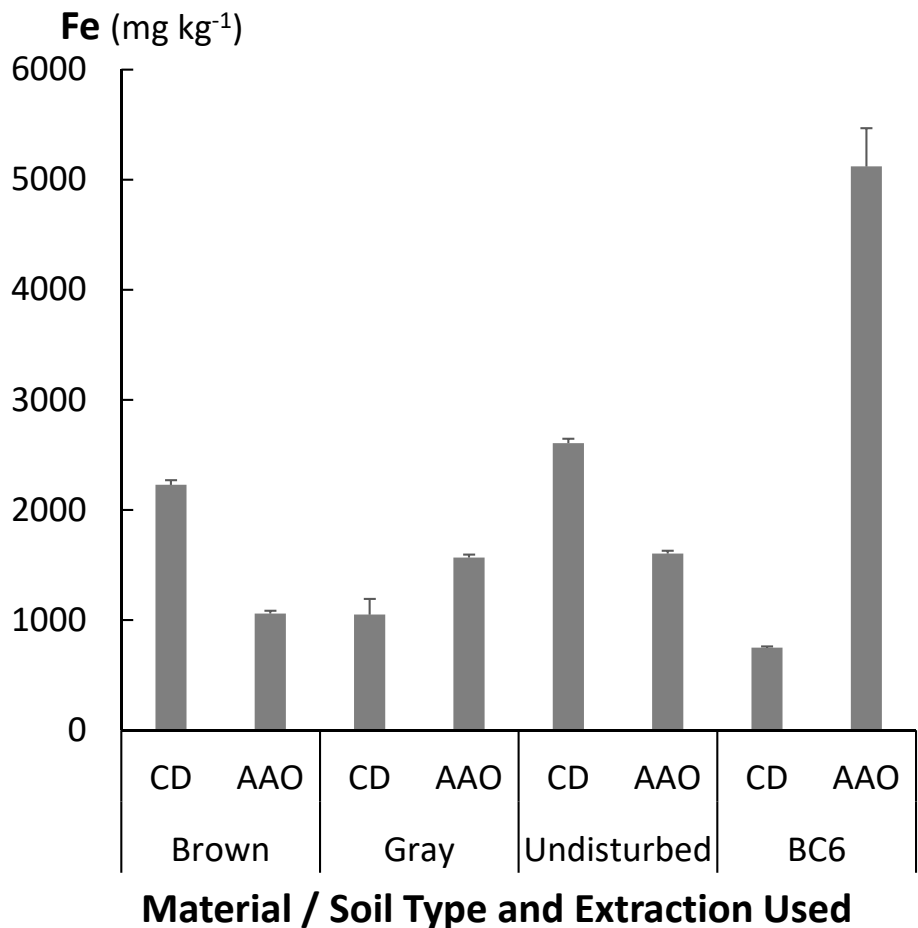


Figure B1. Acid-ammonium-oxalate (AAO) and Citrate-dithionite (CD) extractable iron in the Brown, Gray and undisturbed / native soil and in gray sandstone quarry rock material (vertical lines are one standard deviation).

This trend is highly unusual in soils and can be understood in the context of it being a poorly weathered unconsolidated parent material (e.g. crushed rock in this instance). This is consistent with the results we found for the quarry crushed gray sandstone material (see BC6 in Fig. B1), which represents ‘soil parent material’ of gray sandstone soil. This similarity between the Gray soil and the quarry material are expected given the fact that the gray “soil” is young and of very limited soil development.

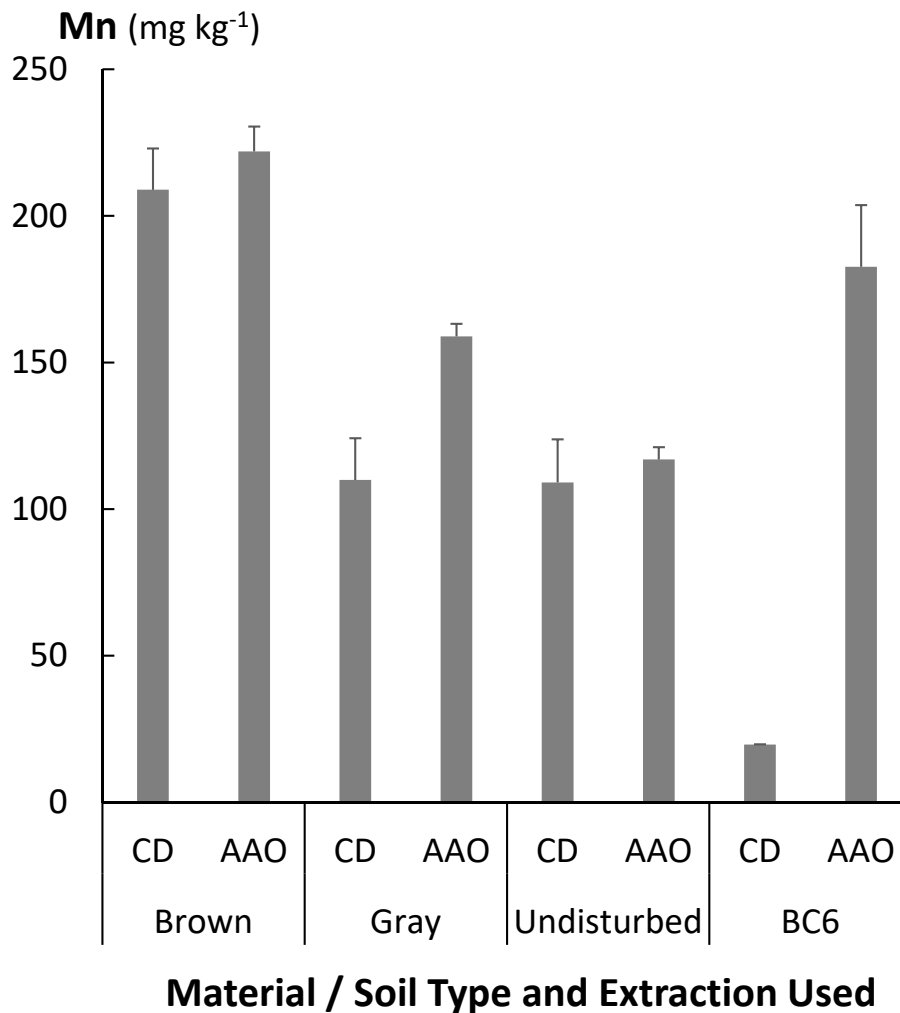


Figure B2. Acid-ammonium-oxalate (AAO) and Citrate-dithionite (CD) extractable manganese in the Brown, Gray and undisturbed / native soil and in gray sandstone quarry rock material (vertical lines are one standard deviation).

AAO and CD-extractable manganese are presented in Figure B2. As in the case of iron, Mn_{CD} was lower than Mn_{AAO} for both the gray soil and sandstone materials. In all, extractable Mn was very low and no significant differences were found between the CD or AAO extractable Mn in the brown or undisturbed soils.

To conclude, the trend of $M_{eAAO} > M_{eCD}$ found here are unusual and inversely related to what is found in well-developed soils. This trend is more conducive to primary minerals behavior and that of parent material or very young soils, which these mine sites are. Findings from these wet-chemistry assays suggests limited pool size of free oxides of iron and/or manganese in both the brown and gray soils. This likely to further imply on limited ability of these soils to support, or buffer for, high redox potential if/when soil gas (air/oxygen) diffusion and fluxes become restricted. Such restricted or limited diffusion/fluxes are intensified in situation and events of excess moisture and/or soil inundation. Compacted conditions will of course limit soil total porosity as well as shifting soil pore size distribution to narrow/smaller size ranges which further limit gas diffusion and exchange. As we observed and report earlier, redox

seemed to play a significant role in solution chemistry and composition in these soil systems and any gas flux / diffusion impairment will further exacerbate such conditions and processes.

Column experiment

To further assess the effect of access moisture and wet/dry cycles on soil solution leachate composition we conducted a column study. Each column was constructed from a 40-cm long 4” PVC pipe. The columns were capped at the bottom which was fitted with 3/8 outlet (later connected to collection cup and vacuum pump). A perforated plastic base was placed at the bottom of the column. The base plate was covered with a nylon mesh (50um opening) and a 0.4 cm layer of silica powder was cemented on top of it. This layer was then covered with 1-cm acid-washed sand and the column was then filled with 30 cm of either brown or gray soil collected earlier from the field sites in early 2017. The soil column was topped with 15 g of forest floor material from the respective sites and covered with 1-cm of acid-washed sand. Each soil was replicated 3 times and the soil columns were subjected to wet/dry cycles using 350mL of DIW. Induced leaching was imposed using a vacuum pump operated at -15KPa ($h_{H_2O} = 153\text{cm}$) either 24 hours after water addition (at the end of a dry cycle) or after the wet period interval. Preset weekly wet/dry intervals had to be extended to assure that the intended conditions indeed develop in the soil columns. The column experiment was initiated on the first week of June 2018 and still continue. In the 53-week period being reported here each column received ca. 44” of DIW, amount similar to the region annual total precipitation.

Selected soil leachate parameters are presented in Figures B3-B6 below. Leachate conductivity decreased over time and was highly dependent on wetting/drying conditions, resulting in a sinusoidal wave-type curve with peaks occurring at the end of wet intervals and bottoms at the end of dry ones (Fig. B3). It is noteworthy that the same volume of water (350 mL) was applied during each period interval and induced leaching event (i.e. dry or wet). The differences being the period of time the water were kept in the column before the induce leaching (residence time; 24 h in the case of dry period – water applied 24 hours prior to ending of a dry interval; or kept in the column throughout a wet interval). Initial results indicate that we were not able to induce the desired drying conditions and as a result the dry period (and later on the wet period) were extended to two or three weeks. The different soils behave similarly in response to the wet/dry conditions, with the gray exhibiting higher EC values than the brown soil throughout the experiment. This occur after initially higher EC values for the brown soil (Fig. B3). While the gray soil experienced EC levels above the $300 \mu\text{S cm}^{-1}$ regulatory threshold, that of the brown neared or exceeded that level only following wet intervals.

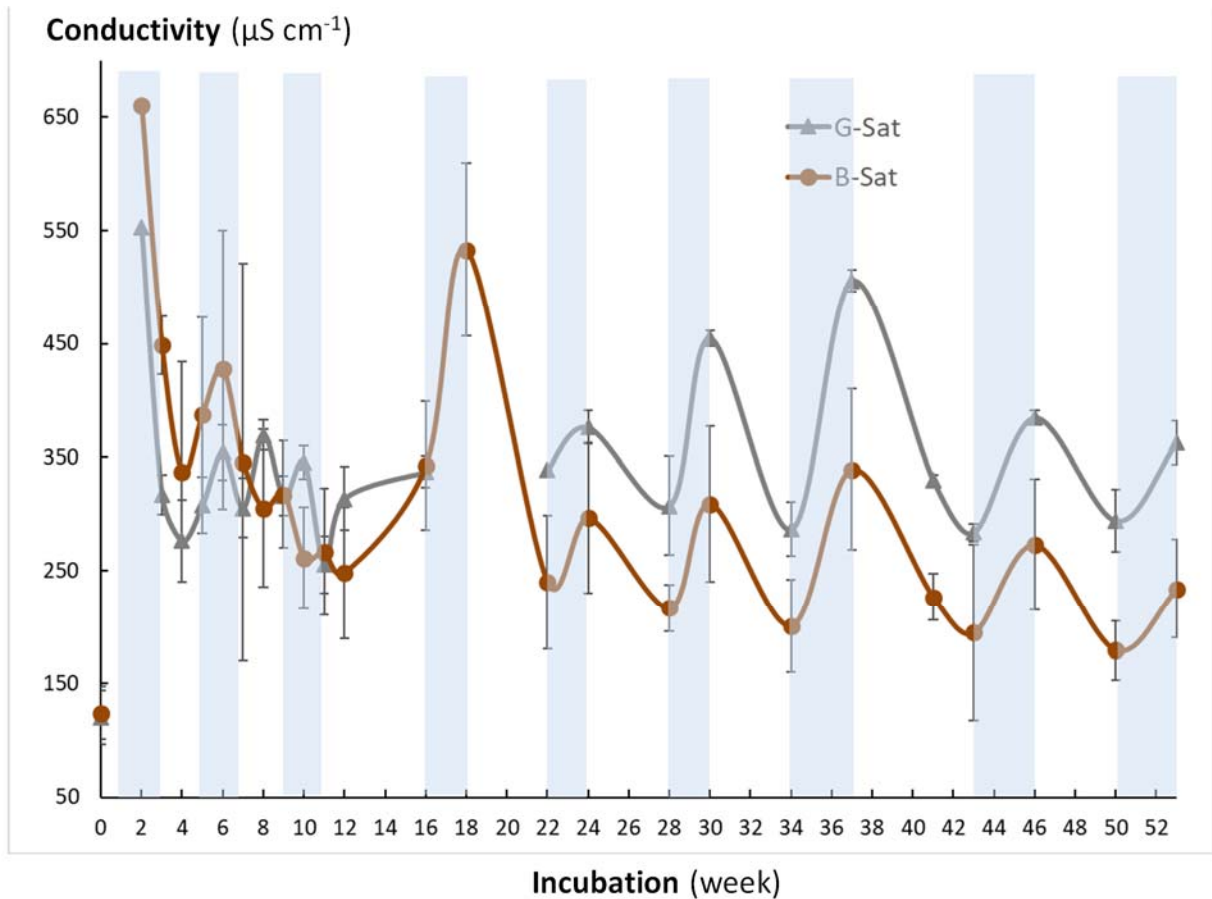


Figure B3. Leachate conductivity in the brown (round symbols) or the Gray (triangular symbols) soil during wet/dry cycles column experiment (shaded column represents wet period; vertical lines are one standard deviation).

Ammonium in the soil leachate followed similar pattern as did conductivity in the brown soil (Fig. B4A) and seemed to be depleted early on in the gray soil (Fig. B4B). Conversely, nitrate seemed to be out of sync with EC in both the brown and the gray soils (Fig. B5). From biogeochemical and redox process considerations, NO_3 can be viewed as an indicator to oxic / anoxic conditions. As such, the increase of nitrate during the dry period is indicative to aerated aerobic conditions whereas the decrease in nitrate during the wet cycle indicate development of anoxic condition and dissimilatory reduction of nitrate to N_2 and/or ammonium (as terminal electron acceptor for energy generation). The initial low levels of nitrate (see the flat line portion of nitrate in Fig. B5A) indicate that the cycle intervals were too tight, preventing development of aerobic conditions during the “dry” interval (these conditions prevailed during these intervals as their duration extended later in the experiment).

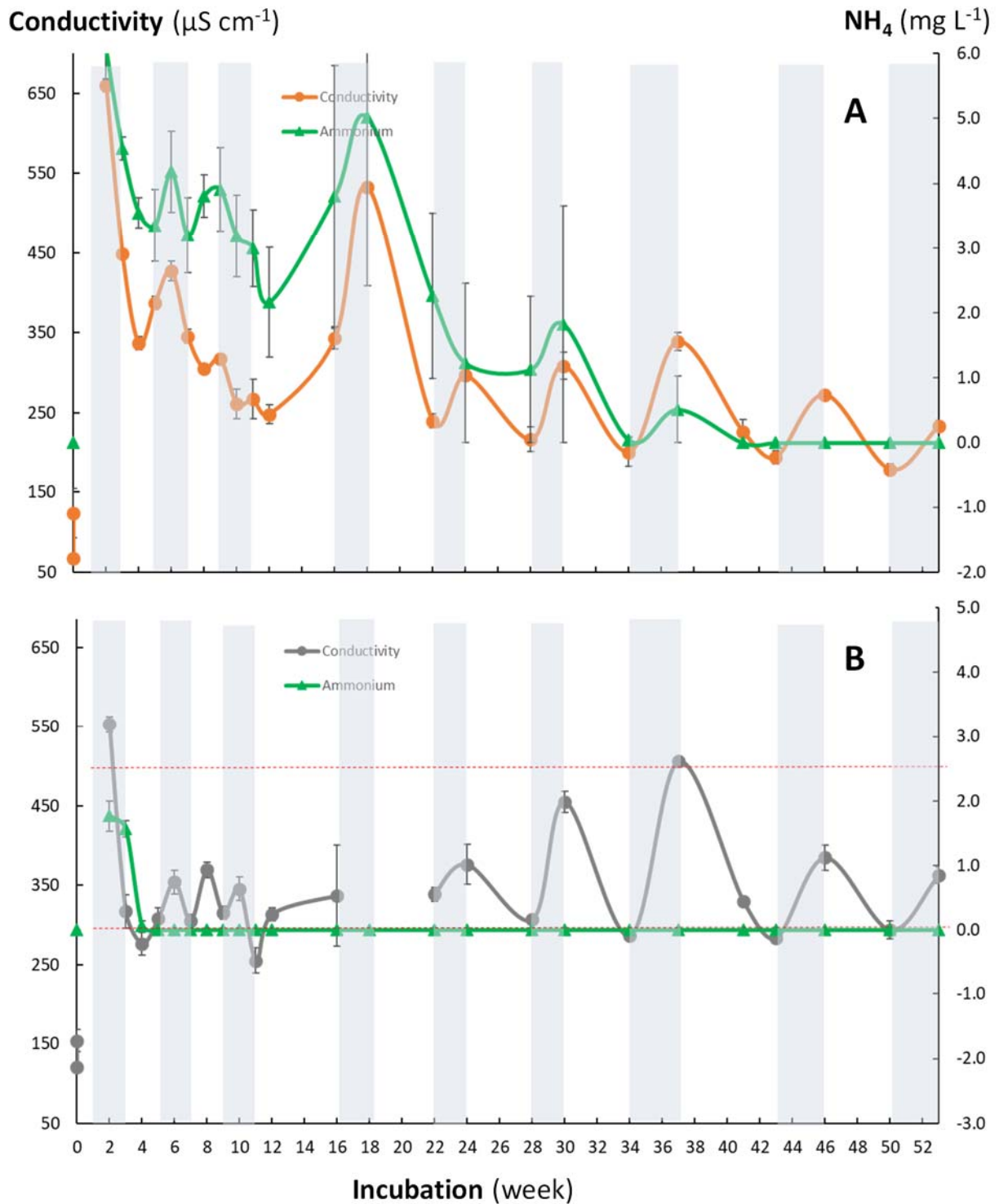


Figure B4. Leachate EC and NH_4 in the brown (A) or Gray (B) soil during wet/dry cycles column experiment (shaded column represents wet period; vertical lines are one standard deviation; dissected red lines represent 500 or 300 $\mu\text{S cm}^{-1}$).

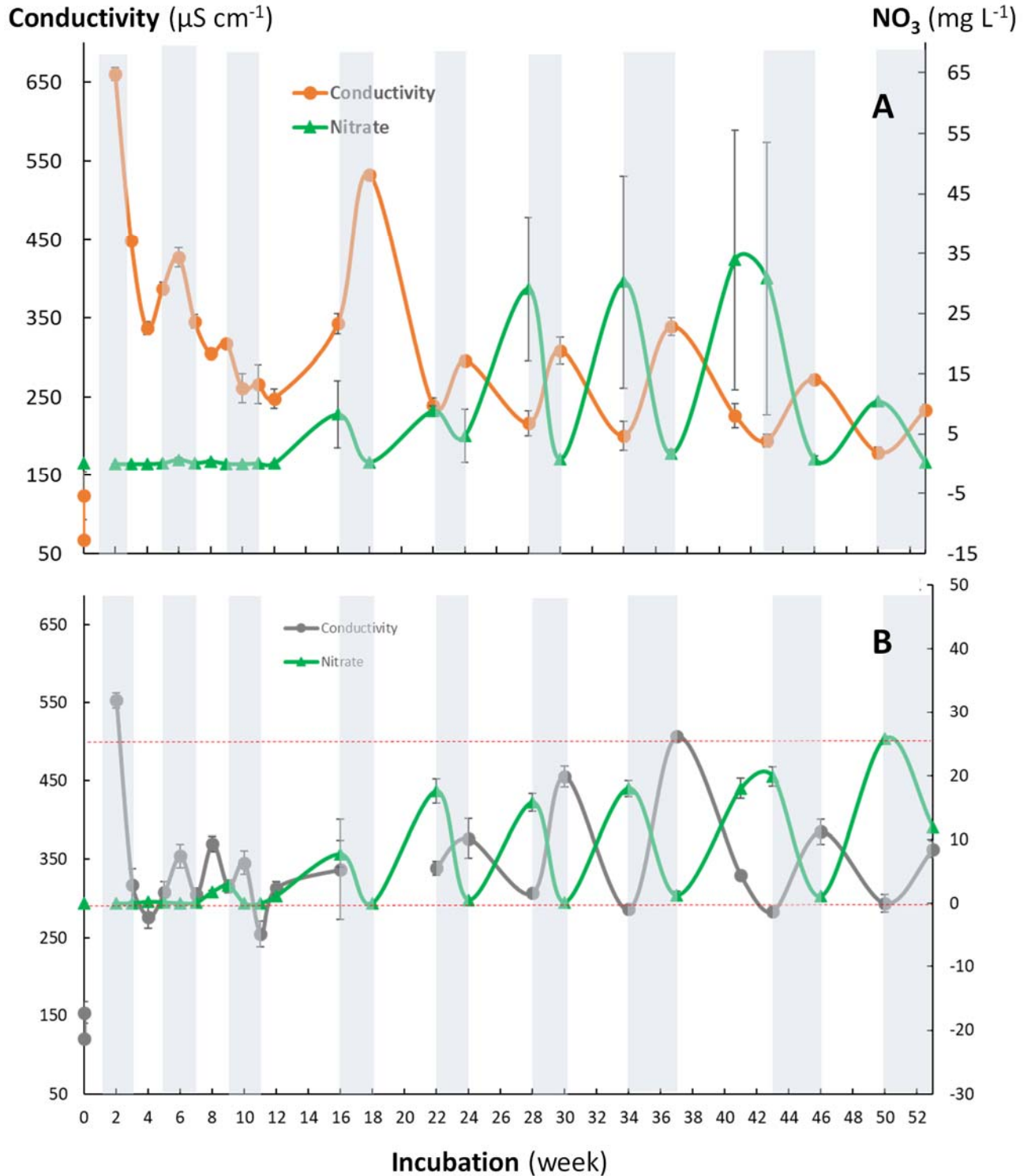


Figure B5. Leachate EC and NO₃ in the brown (A) or Gray (B) soil during wet/dry cycles column experiment (shaded column represents wet period; vertical lines are one standard deviation; dissected red lines represent 500 or 300 $\mu\text{S cm}^{-1}$).

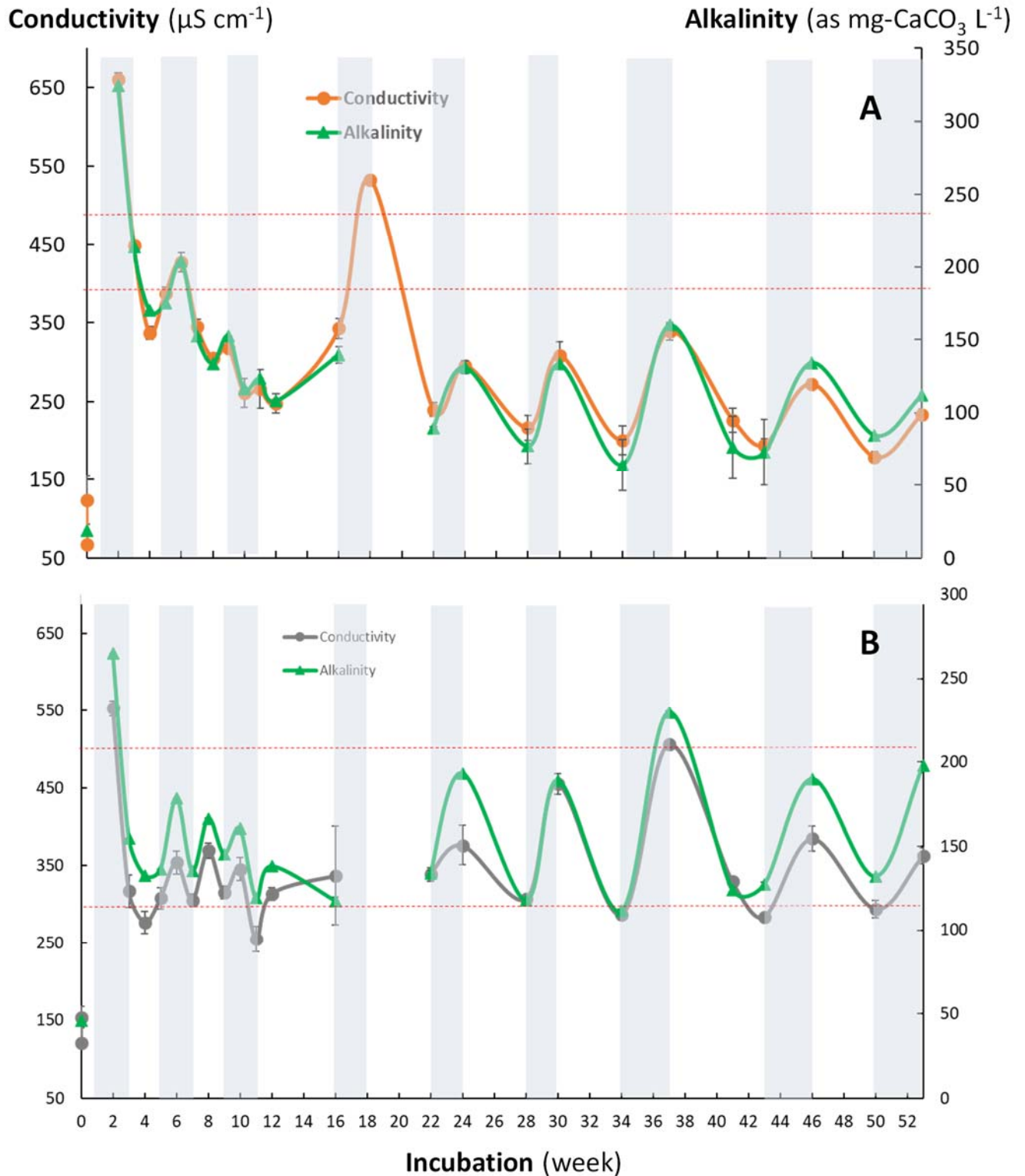


Figure B6. Leachate EC and alkalinity in the brown (A) or Gray (B) soil during wet/dry cycles column experiment (shaded column represents wet period; vertical lines are one standard deviation; dissected red lines represent 500 or 300 $\mu\text{S cm}^{-1}$).

Leachate alkalinity was in sync with EC, increasing during the wet intervals, in both the brown and the gray soils (Fig. B6), exemplifying restricted gas exchange (resulting in increase in CO₂ partial pressure and in dissolved CO₂, and subsequent carbonic acid and speciation thereof as a consequences). Sulfate behaved similarly to alkalinity and EC, increasing it wet intervals and decreasing during dry ones (data not shown). In all, the column experiment showed that the EC of the soil solution/leachate was highly affected by soil wet / dry cycles which were synonymous to anoxic / oxic conditions (as indicated by NH₄ and NO₃ behavior). This further support the field observation, pointing to the dependency of solution EC on redox potential (i.e. oxic/anoxic conditions) and processes. Given the use of spoils as topsoil replacement material, these association of high EC with low redox potential further emphasis the importance of supporting aerated, oxic, aerobic conditions in the soil. Especially given the soil development stage (or lack thereof) of these soils and development of reducible phases / pools. Current FRA practices which assure minimal compaction and support intensive establishment and growth, leading subsequently development of soil organic matter pool, further support management of conditions that support beneficial biogeochemical processes associated and controlling soil (and surface and subsurface) water quality.
